Optimal Back-Off Distribution for Maximum Weighted Throughput in CSMA

Nicola Cordeschi, *Member, IEEE*, Floriano De Rango, *Senior Member, IEEE*, and Andrea Baiocchi

***Abstract*— We consider a generalized version of Carrier-Sense Multiple Access (CSMA), where the contention window size is a constant and the back-off probability distribution can be varied. We address the optimization of a weighted throughput metric, identifying the optimal back-off Probability Density Function (PDF). We give a simple fixed-point algorithm to compute the optimal PDF and prove that the solution is unique. The weighted throughput definition caters for aspects other than the mere channel utilization. It reduces to plain utilization (normalized throughput) when all weights are equal to 1. We also reconnect our result to the classic analysis of saturated non-persistent CSMA, as introduced in the seminal paper by Tobagi and Kleinrock, proving formally that the modeling assumptions of that work, that lead to a Geometric PDF of back-off, actually correspond to the throughput-optimal choice, provided that the ratio of the Geometric PDF is suitably chosen.**

***Index Terms*— CSMA, back-off PDF, throughput optimization, weighted throughput.**

I. Introduction

A LOT of interest has been given to scalable MAC approaches able to present good performance in cases where high node density needs to be supported or where nodes send sporadic, but relevant communication due to some sensed activity, so needing to maximize their success probability.

Carrier-Sense Multiple Access (CSMA) holds a prominent position in the arena of MAC protocols, having been adopted as the primary basis for the channel sharing procedure by most versions of WiFi, by sensors networks (e.g., IEEE 802.11ah), by vehicular networks (e.g., IEEE 802.11p/bd), and RFID networks. Optimizing CSMA algorithms has been intensely investigated.

Quite interesting contributions based on CSMA/CA techniques for WSN or RFID systems [1], [2] have been proposed. Some extensions of these techniques have been integrated into industrial delay-sensitive control networks, monitoring applications, IoT over WiFi or vehicular networks [3], [4], [5], [6]. A recent trend about MAC strategies is focusing on protocols where contending nodes do not change the Contention Window (CW) after collisions, but rather dynamically change the contention probability to improve the success probability or the throughput [7], [8]. Even in this case, it is crucial to set carefully the CW size and the contention probability. Both the performance and the optimized CW size of these approaches can be too sensitive to the number of nodes, making them suitable for limited communication range and low deployment densities, but not performing well in massive high-density scenarios.

To face these problems, CSMA back-off policies based on a slotted fixed window with uniform and non-uniform attempt probability distributions have been proposed in [1], [8], [9], and [10].

Throughput and delay performance of these approaches are almost independent of the number of contenders, achieving simplicity and good throughput under both low and high contention levels, so promoting these techniques as suitable for massive IoT and high-density WSN [11].

In this paper we derive the optimal back-off Probability Density Function (PDF) of a CSMA protocol with fixed contention size so as to maximize a notion of generalized weighted throughput, which reduces to plain channel utilization (also referred to as normalized throughput in the following) when all weights are equal to 1. Specifically, the optimal PDF is derived for the case where all contention slots are uniformly weighted, which leads to the classic notion of normalized throughput, and under the condition where slots can have different weights to match different application contexts. As a matter of example, energy-constrained scenarios require to reduce the contention time, and this is obtained by weighting more lower index back-off slots, i.e., stations get a higher reward if access is attempted early. To the best of our knowledge, no work focused on the optimal PDF able to maximize the (weighted) throughput.

We define a unified framework, encompassing limited contention window size (so called 'no skip' option) as well as the possibility of having unlimited contention window size ('skip' option). We derive a fixed point algorithm yielding the optimal back-off PDF under any contention window size, and any set of weights. It is proved that the fixed point iteration converges to a unique solution.

We also reconnect our result to the classic analysis of saturated non-persistent CSMA, as introduced in the seminal

Manuscript received 22 December 2022; revised 3 August 2023 and 29 December 2023; accepted 10 March 2024; approved by IEEE/ACM TRANSACTIONS ON NETWORKING Editor R. Vaze. Date of publication 12 April 2024; date of current version 20 August 2024. *(Corresponding author: Nicola Cordeschi.)*

Nicola Cordeschi is with the Department of Electric and Information Engineering (DEI), Polytechnic University of Bari, 70126 Bari, Italy (e-mail: nicola.cordeschi@poliba.it).

Floriano De Rango is with the Department of Informatics, Modeling, Electronic and Systems (DIMES), University of Calabria, 87036 Arcavacata, Italy (e-mail: derango@dimes.unical.it).

Andrea Baiocchi is with the Department of Information Engineering, Electronics and Telecommunications (DIET), Sapienza University of Rome, 00185 Rome, Italy (e-mail: andrea.baiocchi@uniroma1.it).

Digital Object Identifier 10.1109/TNET.2024.3387322

paper by Tobagi and Kleinrock [12], proving formally that the modeling assumptions of that work, that lead to a Geometric PDF of back-off, actually correspond to the best possible choice (i.e., the one maximizing channel utilization), provided that the ratio of the Geometric PDF is suitably chosen.

The paper is organized as follows. Section II reviews the related literature. Our proposed system model along with the main assumptions and notation is detailed in Section III. Section IV presents main results, stating the fixed-point algorithms with uniform and not uniform weighted throughput. Numerical and simulation results are given in Section V. Finally, conclusions are presented in Section VI. Mathematical details and proofs are postponed to a dedicated Appendix.

II. Related Work

Many works have been proposed in literature to consider scalable MAC strategies able to maintain good performance even under high-density network scenarios [13], [14]. Some of these works considered also situations where it is hard to get accurate estimates of node density due to multiple network events such as link-failures, node mobility, sleep mode strategies [15]. In these cases, knowing theoretical bounds on MAC performance in terms of throughput can be a key point, especially to compare or integrate different technologies such as new generations of wireless interfaces (WiFi) [16], [17], [18].

CSMA plays a prominent role in the realm of wireless multiple access. Several variants of CSMA have been employed, e.g., CSMA with Collision Avoidance (CSMA/CA) is the cornerstone of the MAC protocol defined for the WiFi. Variants of the basic CSMA/CA are also used in sensor networks (e.g., IEEE 802.15.4) or RFID networks [9], [19]. The success of CSMA and the ensuing wide availability of low-cost chipsets is a strong motivation to continue referring to this technology, while trying to improve its performance especially with growing number of nodes.

Analysis and optimization of throughput in CSMA networks has been intensely investigated, since the seminal paper of Tobagi and Kleinrock [12] and the analysis of CSMA/CA in Bianchi's work [20]. Also more general optimization problems have been addressed, e.g., optimization of throughput and energy consumption [14], [21].

Two major approaches can be identified to the optimization of CSMA throughput.

A first group of works follows the CSMA/CA approach and propose ways to set the contention window size to optimize the throughput, while the back-off probability distribution is uniform [19], [22], [23], [24], [25], [26], [27], [28]. An adaptive algorithm to tune the contention window size to its optimal value is given in [24]. The proposed algorithm is consistent with IEEE 802.11 CSMA/CA. It is based on the estimate of the number of consecutive idle back-off slots between two consecutive packet transmissions. Optimal throughput is achieved by properly setting the target contention window size, as a function of the number of contending stations. Other adaptation algorithm for setting the contention window size at an optimal level are given in [25] and [26]. More recently, machine learning and reinforcement learning approaches have been considered as well, to adapt the contention window size of CSMA/CA in IEEE 802.11 and thus to steer the protocol towards optimized performance, e.g., see [27] and [28]. Summarizing, the first group of works generally follows a Distributed Coordination Function (DCF)-like CSMA/CA approach. They adjust the initial backoff window size or control the amount of traffic entering the network, by proposing some modifications to the scheme implemented by the IEEE 802.X families. This strategy is notoriously short-term unfair, with long transients before reaching convergence and too sensitive to the number of nodes [16], [18]. These impairments make these approaches generally useful for limited communication range and low deployment densities, but not in massive high-density scenarios. In addition, they do not relate the access parameters to the optimization metrics in a straightforward way prone to flexible optimized solutions.

An alternative approach, closely related to the variable contention window size optimization, is state the CSMA model in terms of transmission probability of a backlogged node. Then, the transmission probability is set so as to optimize the throughput [20], [29], [30], [31]. A key assumption of those works is that the attempt rate of all other nodes from the point of view of a tagged node is a constant. This assumptions is consistent with assuming that a Geometric probability distribution of the back-off duration.

Calì et al. [29] analyze CSMA from the standpoint of throughput. They propose replacing the uniform-distribution contention window of 802.11 with a p-persistent back-off protocol [29]. By estimating the population size, they maximize system throughput when all nodes always have a packet ready for transmission. They show that 802.11 yields sub-optimal throughput under this workload. A fixed point equation yielding the optimal transmission probability is determined in [20]. There is a strict connection between the optimal transmission probability τ^* and the optimal contention window size W^*, at least in a symmetric case (statistically equivalent nodes). Namely, $\tau^* = 2/(1 + W^*)$ relates the expressions of the saturation throughput obtained in the two cases.

A second group of works considers a fixed contention window size and tries to find suitable back-off probability distributions to improve CSMA performance [8], [9], [11], [32], [33], [34]. Cai et al. [32] propose a polynomial distribution for non-persistent CSMA contention slot selection. Their distribution is optimal over the space of all polynomial functions, whereas ours is optimal over the space of all probability density functions. An in-depth analysis of the fixed point equation yielding the optimal transmission probability of CSMA is presented in [30] and [31]. This works follow the classic model of CSMA/CA, where it is assumed that a backlogged station attempts transmission with a fixed probability after sensing an idle back-off slot, i.e., the probability distribution of back-off is Geometric. While the optimal transmission probability is found, there is no proof that the Geometric PDF of back-off need necessarily be the best choice for throughput. In [8] a non-uniform CSMA distribution able to reduce the latency for the delivery of event reports has been proposed. The scheme needs to estimate the total number of contenders in the network and is not

optimal in terms of throughput. In [9] authors propose a Geometric Distribution Reader Anti-collision (GDRA) where RFID readers used a truncated geometric distribution function to select a contention slot, instead of the typical uniform distribution function. Also approaches merging contention window adaptation (or robustness to such a change) and non-uniform PDFs have been proposed. Authors in [33] propose a priority control method using non-uniform backoff probability density to accommodate different performance metrics, such as latency or throughput, based on the application requirements. A Binary Exponential Backoff (BEB) has been applied in [34], where nodes intelligently determines overlapped contention slots and probabilistically minimizes their selection chances. Authors replace the classical uniform distribution in the BEB with a dynamic non-uniform distribution, able to increase the system throughput also reducing the delay for increasing number of stations. In [11] a slotted non-persistent CSMA/CA with nonuniform contention probability distribution has been proposed, designed to reduce at the same time latency of contenders and preserve a high successful access probability. It is shown to be insensitive to the number of contenders and very robust with respect to contention window size, packet length, and impairments such as frame synchronization errors.

The examined works give useful insights into the need to devise CSMA/CA strategies able to manage different targets in a flexible way, and the possibilities provided by non-uniform probability densities to pursue this goal.

Our work belongs to this second group of approaches. In a nutshell, our model and analysis can accommodate a family of metrics wider than the traditional channel utilization, providing the optimal PDF through a simple fixed point algorithm. Noticeably, we highlight that the optimality results we obtain are new even under the scope of traditional normalized throughput.

More in dept, a general framework is defined for a CSMA network, where the back-off probability distribution can be arbitrary, while the contention window size is fixed. We cover both the cases of a finite contention window size and inifinite size. The latter is obtained by introducing a model parameter (the skip variable), that allows the contention window size to extend without limits. We use the back-off probability distribution as the degree of freedom to optimize CSMA throughput, providing a fixed point algorithm to compute the optimal back-off PDF for each given number of contending stations. Our general framework also solves a long-standing issue, i.e., we can prove formally the optimality of the widely used Geometric PDF for back-off. Moreover, it lends itself to encompass in a unique optimization framework additional requirements to be traded-off with respect to throughput optimization, thanks to the notion of weighted throughput. We present an example of this feature of our modeling approach in Section V-B. Those are the main new contributions that we propose, with respect to existing literature.

III. System Model and Analysis

In this section we introduce the modeling assumptions and the notation used in the paper (Section III-A). Then, we derive the expression of the saturation throughput in Section III-B, introducing a notion of weighted throughput that generalizes the usual normalized throughput definition.

The main result of the paper, the derivation of the PDF of back-off countdown that maximizes the weighted throughput, is presented in Section IV.

A. Assumptions and Notation

The considered CSMA framework is a generalization of non-persistent CSMA, where a general PDF for the back-off count is allowed, i.e., the number of back-off slot times to be counted down by a backlogged contending station is drawn according to a general PDF, to be defined according to a specific target, e.g., throughput maximization.

We consider n stations sharing the wireless channel, and we make the usual assumptions established since Bianchi's seminal work [20]:

- stations are saturated, i.e., they always have packets ready to send;
- stations can hear each other, i.e., there is no hidden station.

As a consequence of these assumptions, all stations see the same channel status. To keep notation simple and gain the most insight provided by models, we also assume that unlimited retransmission is allowed and that channel holding time is the same for all stations, once they win the contention.

Let us now outline the contention procedure adopted by a station.

As soon as the channel gets back to idle after a transmission, the station waits for the channel to stay idle for a fixed time (Inter-Frame Space (IFS)). We identify this time with the back-off slot time, denoted with δ, without loss of generality. Then, the station draws an integer value k with probability q_k, with $1 \leq k \leq m$. The set of probabilities $\{q_k\}_{1\leq k\leq m}$ is referred to as the back-off probability distribution. The number $m \geq 2$ is the contention round (CR) length, also referred to as the contention window size. A back-off counter is initialized to $k-1$ and the transmission countdown starts. The station decrements the back-off counter at the end of the current back-off slot time, if the channel is sensed as idle during that back-off slot time. The countdown continues until the counter hits 0. When the counter hits 0, the station starts transmitting. The channel is then held busy for a time that includes transmission of one or more packets, inter-frame spaces and possibly an acknowledgment. We do not enter the details of the MAC packet format and timing, rather we define an overall transmission time T, encompassing all activities performed by a station when it wins the channel.

If during the countdown another transmission starts, the station whose countdown has been interrupted by the start of another transmission deems itself as having lost the contention, resets its counter, waits for the end of the transmission. When the transmission ends and the channel gets back to the idle state, the station repeats the whole procedure anew, i.e., it draws another independent value of the random counter and starts a fresh new countdown.

Note that a collision event occurs whenever two or more stations draw the same initial back-off counter value and all

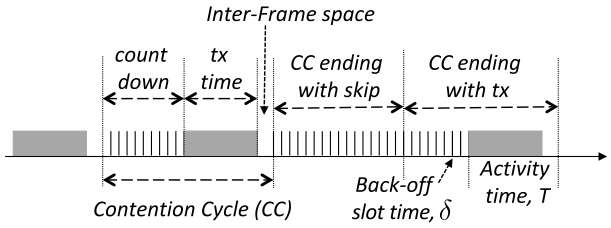

Fig. 1. Example of time evolution of the generalized CSMA defined in Section III-A. Examples of both Contention Cycles without and with skip are shown on the right of the diagram. The CC ending with a skip comprises $m = 16$ back-off slot times and no transmission. The ensuing CC is composed of 8 back-off slot times, after which one or more stations start transmitting.

other stations draw a bigger back-off counter value. As a matter of example, if there are four contending stations and two of them draw $k = 3$, while the other two stations draw $k > 3$, the first two stations will count off $(k - 1) = 2$ idle back-off slot times after the IFS, and then they will start transmitting, thus ending up into a collision at slot $k = 3$.

As a consequence of the proposed back-off procedure, the time evolution of the channel is split in *contention cycles* (CCs). A CC consists of a contention round (CR), possibly followed by an activity time (AT). CR consists of a number of consecutive idle back-off slot times, whereas AT lasts a time T. Figure 1 illustrates an example of time evolution of the CSMA protocol described in this section. On the right of the figure, two consecutive CCs are shown, the first one ending with a skip (no transmission attempt takes place, after all $m = 16$ back-off slot times have been counted off), the second one ending with a transmission attempt.

The slotted non-persistent CSMA introduced in the classic paper of Kleinrock and Tobagi [12] corresponds to the contention procedure described so far with the special choice $m = \infty$ and Geometric PDF for the back-off counter k. The CSMA/CA procedure defined in WiFi assumes a uniform probability distribution for the back-off counter. Moreover, a backlogged node freezes its counter in case its countdown is interrupted by other nodes' transmissions. In that case, the node checks the channel until transmission is over and the channel is sensed back to idle state. At that point, the node resumes the countdown. Eventually, the countdown expires and the node does transmit. If successful, the node is done and can move on to the next backlogged packet. If instead the node runs into a collision, Binary Exponential Back-off is used, i.e., the countdown window size is doubled before drawing the new initial countdown value.

We will see that giving up to BEB, the simpler Geometric PDF for the initial countdown selection turns out to optimize the channel utilization (i.e., normalized throughput). In other words, a higher saturation throughput can be achieved, if stations follow a simpler scheme, where a new initial countdown value is selected always from the same (Geometric) PDF, irrespective of the number of (re-)transmission attempts for the same packet. We will prove that a similar result applies when the more general weighted throughput function is introduced. In that case, not even the Geometric PDF is optimal. Nevertheless, our approach is able to derive the optimal scheme, customized to the given target. Moreover, our approach lends itself to throughput optimization also in the case where a constraint is set on the mximum back-off window, i.e., by considering finite support back-off probability distributions.

The multiple access algorithm defined so far corresponds to the contention procedure described in Section II of [1]. We extend it now by considering a modified probability distribution over $m + 1$ values, namely $\{q_i\}_{1 \le i \le m+1}$. The algorithm remains as stated before, except that a station drawing the value $m + 1$ *skips* the current contention cycle, without competing, i.e., it gives up the contention for the current cycle. Hence, a contention cycle ends: (i) when one or more stations start transmitting having hit 0 with their counters (initialized at values $k \le m$); or (ii) when m idle back-off slots go by on the channel and no transmission starts (i.e., all backlogged stations have chosen the skip option). Whichever of the two events occurs first will determine the end of the current CC. As soon as the CC ends, each backlogged station draws another random value to initialize its counter and enters a new CC.

The motivation of the skip option is as follows. Variability of the access delay implied by non persistent CSMA can be mitigated by setting a limit to the maximum number of back-off slot times to be counted down before attempting transmission. This is done, e.g., by choosing a uniform back-off PDF over the interval $[1, m]$, as done in WiFi. Questions we aim to answer in this paper are then: (i) How far is uniform probability distribution from the optimal back-off PDF? (ii) How does the optimal back-off PDF with a given contention window length m look like? A further question that arises after having introduced the optimal back-off PDF with a limited contention window size is: How much is a maximum contention window length m penalizing in terms of throughput? In other words, we aim to assess the potential throughput gain obtained by relaxing the constraint on the maximum number of back-off slot times m. To embrace this analysis in the same modeling framework used for finite contention window length m, we introduced the skip option, which essentially means extending the contention window length to ∞.

In this paper we derive the optimal probability distributions maximizing the system throughput for both cases with and without skip option. To use a common framework and notation, we denote by s a $0/1$ skip flag. Specifically, if $s = 0$ the skip is not allowed, and q_{m+1} is set to 0 as a constraint. Vice versa, if $s = 1$ the skip is allowed and the skip probability q_{m+1} is left as an output of the optimizer. An example of a CC with skip is shown in Figure 1.

Table I summarizes the main notation used in the paper.

B. Derivation of Throughput

Regardless of selected strategy $s = 0/1$, in order to derive an expression of the system throughput, let $K(\ell)$ denote the random variable representing the countdown value drawn by station ℓ at the beginning of a new contention cycle. The random variables $K(1), \ldots, K(n)$ are i.i.d., namely $K(\ell) \sim K$, $\forall \ell$, and $q_k = \mathcal{P}(K = k)$ for $k = 1, \ldots, m+1$. The random

TABLE I
MAIN NOTATION USED IN THE PAPER

Symbol	Meaning
n	Number of stations.
δ	Duration of back-off slot time.
T	Duration of activity time, i.e., time required for a station seizing the channel to complete its operations (packet transmission, ACK reception, inter-frame spacing).
β	Normalized back-off slot time, $\beta = \delta/T$.
m	Contention window size.
K	Discrete random variable taking values in $\{1,\dots,m+1\}$. It represents the initial back-off counter value at the beginning of each Contention Cycle (CC). The special value $K = m+1$ means that the station skips the current CC.
s	Binary variable determining whether skip is enabled ($s = 1$) or not ($s = 0$). $K = m+1$ is allowed only if $s = 1$.
$K(\ell)$	Value of K drawn by station $\ell = 1,\dots,n$.
C	Random variable representing the number of backoff slot times counted down during one Contention Cycle.
q_j	Probability to choose $K = j$, for $j = 1,\dots,m+1$.
F_j	Probability that $K \le j,\ j = 1,\dots,m+1$. For ease of notation, we let also $F_0 = 0$.
G_j	Probability that $K \ge j,\ j = 1,\dots,m+1$. For ease of notation, we let also $G_{m+2} = 0$.
τ_j	Probability that a station starts transmitting on the idle back-off slot time j, given that it backed off for the previous $j-1$ idle backoff slot times.
α_j	Weight of realized throughput, given that transmission occurs immediately after the $(j-1)$-th idle back-off slot.
$P_s(n)$	Probability of a CC ending with a successful transmission (i.e., exactly one attempt out of the possible n ones)
ρ_n	Normalized saturation throughput (aka channel utilization) for n stations, defined as the mean fraction of time that the channel is used successfully.
$\rho_n^{(\alpha)}$	Weighted throughput for n stations, as defined in Equation (6).

variable K takes values in $\{1,\dots,m+1\}$, where the special value $K = m+1$ means that the station skips the current contention round.

The number of idle back-off slot times making up a contention round is $J = \min\{m, \min\{K(1),\dots,K(n)\}\}$. At the end of the contention round, either all stations choose to skip transmission or at least one station transmits. The former event is only possible if $\min\{K(1),\dots,K(n)\} = m+1$. If instead $\min\{K(1),\dots,K(n)\} \le m$, an AT follows the CR.

Let C be the duration of a CC, δ the back-off slot time, T the duration of the AT. We have[1]

$$C = \begin{cases} J\delta + T & \text{if at least one station transmits,} \\ m\delta & \text{otherwise.} \end{cases} \tag{1}$$

Let F_j and G_j, for $j = 1,\dots,m+1$, denote the Cumulative Distribution Function (CDF) and Complementary Cumulative Distribution Function (CCDF) of the random variable K, i.e., $F_j = \mathcal{P}(K \le j) = \sum_{i=1}^{j} q_i$, and $G_j = \mathcal{P}(K \ge j) = \sum_{i=j}^{m+1} q_i$. It is $F_{m+1} = 1$ and $G_1 = 1$. For ease of notation we also define $F_0 = 0$ and $G_{m+2} = 0$. Then, we have $F_j + G_{j+1} = 1,\ j = 0,\dots,m+1$.

[1]More generally, stations wait for the channel to stay idle for an IFS $> \delta$ before starting the new CR. However, this does not affect our analysis and derivations, since the fixed duration (IFS $-\delta$) can be embedded as an additive constant into the first line of Equation (1) (and, consequently, embedded in T). We choose IFS $= \delta$ for simplicity.

The probability of a CC ending with a successful transmission (i.e., exactly one attempt out of the possible n ones) is

$$P_s(n) = \sum_{i=1}^{m} n q_i G_{i+1}^{n-1} = \sum_{i=1}^{m} n q_i (1-F_i)^{n-1} \tag{2}$$

The mean duration of a CC is

$$\mathrm{E}[C] = (\delta\,\mathrm{E}[J \mid \mathcal{E}] + T)\,\mathcal{P}(\mathcal{E}) + m\delta\,[1 - \mathcal{P}(\mathcal{E})] \tag{3}$$

where $\mathcal{E}$ is the event "at least one station transmits in this cycle". We have

$$\mathcal{P}(\mathcal{E}) = 1 - q_{m+1}^n = 1 - G_{m+1}^n = 1 - (1-F_m)^n \tag{4}$$

and

$$\mathrm{E}[J \mid \mathcal{E}] = \sum_{i=1}^{m} i \frac{G_i^n - G_{i+1}^n}{1 - G_{m+1}^n} = \frac{\sum_{i=1}^{m} G_i^n - m G_{m+1}^n}{1 - G_{m+1}^n}$$

where we have used the two identities $G_{m+1} = q_{m+1}$ and $G_1 = 1$. Putting pieces together, we get

$$\begin{aligned} \mathrm{E}[C] &= \delta \sum_{i=1}^{m} G_i^n - m\delta G_{m+1}^n + T(1 - G_{m+1}^n) + m\delta G_{m+1}^n \\ &= \delta \sum_{i=1}^{m} G_i^n + T(1 - G_{m+1}^n) \end{aligned}$$

The normalized saturation throughput, briefly referred to as simply throughput in the following, is defined by the mean fraction of time that the channel is used for successful transmissions. It is expressed as follows

$$\rho_n = \frac{T P_s(n)}{\mathrm{E}[C]} = \frac{n \sum_{i=1}^{m} q_i G_{i+1}^{n-1}}{1 - G_{m+1}^n + \beta \sum_{i=1}^{m} G_i^n} \tag{5}$$

where $\beta = \delta/T$. Given β, n and m, ρ_n is a function of the back-off PDF $\{q_j\}_{1 \le j \le m+1}$.

We introduce also the notion of *weighted* saturation throughput of the n nodes, expressed as follows:

$$\rho_n^{(\boldsymbol{\alpha})} = \frac{T P_s^{(\alpha)}(n)}{\mathrm{E}[C]} = \frac{n \sum_{i=1}^{m} \alpha_i q_i G_{i+1}^{n-1}}{1 - G_{m+1}^n + \beta \sum_{i=1}^{m} G_i^n} \tag{6}$$

where $P_s^{(\alpha)}(n) \triangleq n \sum_{i=1}^{m} \alpha_i q_i G_{i+1}^{n-1}$ is the weighted probability of success. In Equation (6), $\alpha_j \ge 0$ is the reward obtained by a station winning the contention at slot j. The meaning of α_j is application dependent (e.g., see Section V-B).[2]

Due to its versatility, in this section we aim at maximizing Equation (6). Note that for $\alpha_1 = \alpha_2 = \cdots = \alpha_m = 1$ the weighted throughput reduces to the plain throughput in Equation (5), just accounting for channel utilization.

Before proceeding to derive the optimal PDF, we recall a well-known back-off PDF commonly used in literature. Let the back-off PDF be Geometric with ratio $1-\tau$, namely $q_i = (1-\tau)^{i-1}\tau$, $i = 1,\dots,m$, and $q_{m+1} = (1-\tau)^m$. Let us also confine ourselves to the case of non-weighted

[2]Throughout the paper, for the reward weight vector $\boldsymbol{\alpha} \triangleq [\alpha_1,\dots,\alpha_m]$ we assume $\boldsymbol{\alpha} \in (\mathbb{R}_0^+)^m - \{\mathbf{0}_m\}$, unless otherwise specified. For the null weight vector $\mathbf{0}_m \triangleq [0,0,\dots,0]$, the weighted throughput (25) is identically zero and the optimization is trivial.

throughput ($\alpha_j = 1, \forall j$). After some calculations, it is found from Equation (5) that

$$\rho_{n,\mathrm{G}} = \frac{n\tau(1-\tau)^{n-1}}{1+\beta-(1-\tau)^n} \tag{7}$$

regardless of m, which is consistent with the memoryless property of the Geometric PDF. This last expression is reminiscent of the saturation throughput expression holding for CSMA/CA models [12], [20]. More in depth, according to Bianchi's model of CSMA/CA of WiFi [20], the saturation throughput in a symmetric network, as assumed here, is expressed just as in Equation (7). Bianchi's model is known to provides highly accurate predictions of saturated throughput, at least in the parameter value range of interest to CSMA/CA of WiFi. In [20], τ is found as the unique solution (fixed point) of the equation system:

$$\tau = \frac{1+p+p^2+\cdots+p^{\nu}}{\kappa_0+\kappa_1 p+\cdots+\kappa_{\nu}p^{\nu}} \tag{8}$$

$$p = 1-(1-\tau)^{n-1} \tag{9}$$

where ν is the maximum number of allowed re-transmissions, $\kappa_j = (W_j+1)/2$ and $W_j = \min\{CW_{\max}, CW_{\min}\cdot 2^j\}$ is the contention window size at stage j of the binary exponential back-off algorithm, $j = 0, 1, \ldots, \nu$. In the original Bianchi's model it is $\nu = \infty$ and $CW_{\max} = \infty$. In that case, Equation (8) simplifies to

$$\tau = \frac{2}{1+CW_{\min}\dfrac{1-p}{1-2p}} \tag{10}$$

where $CW_{\min}$ is the base contention window size. The throughput achieved by CSMA/CA of WiFi is largely sub-optimal, especially as n grows.

IV. Optimization of Weighted Throughput

In this section we address the identification of the PDF $\{q_j\}_{1\le j\le m+1}$ that maximizes the weighted throughput for n stations, referred to as the optimal PDF. In the following, we denote by τ_j the hazard rate of the back-off PDF, i.e., $\tau_j = \mathcal{P}(K = j \,|\, K \ge j)$. We can view τ_j as the probability that a backlogged station transmits at slot j, conditional on being silent in the previous (idle) $j-1$ slots. Given its definition, we can relate τ_j to the PDF and CDF of the back-off counter K as follows:

$$\tau_j = \frac{q_j}{1-F_{j-1}}, \quad j = 1, \ldots, m. \tag{11}$$

For $n = 1$ the optimal PDF is obviously given by $q_{j^*} = 1$ and $q_j = 0$ for $j \ne j^*$, with j^* given by

$$j^* = \underset{j=1,\ldots,m}{\operatorname{argmax}} \left\{ \frac{\alpha_j}{j\beta+1} \right\} \tag{12}$$

In the following we assume therefore $n \ge 2$.

The main result is summarized in the following theorem. We refer to appendices for the detailed proof.

Theorem 1: For any given $n \ge 2$, $s \in \{0,1\}$, $m \ge 2-s$ and non-negative weights α_j, $j = 1, \ldots, m$, the PDF $\{q_j\}_{1\le j\le m+1}$ of backoff countdown that maximizes the weighted throughput in Equation (6) is obtained according to Algorithm 1, where ε is the desired numerical accuracy.

Before proceeding, let us provide some insight about Algorithm 1 and the rationale behind it. Specifically, Algorithm 1 define an iteration of the form

$$\begin{cases} \nu_k = \Psi_{\boldsymbol{\alpha}}(\nu_{k-1}) & k \ge 1 \\ \nu_0 = 0 \end{cases} \tag{13}$$

k being the iteration index, with starting value $\nu_0 = 0$ (Algorithm 1 line 2), where the function $\Psi_{\boldsymbol{\alpha}}(\cdot)$ is a continuous map of $[0, \alpha_{\max}]$ into itself, with $\alpha_{\max} = \max_j\{\alpha_j\}$. Specifically, for any ν_k entering the $\Psi_{\boldsymbol{\alpha}}(\cdot)$ computation (at Algorithm 1 lines 7 and 9), a PDF

$$\boldsymbol{q}(\nu_k) \triangleq \{q_j(\nu_k)\}_{1\le j\le m+1} \tag{14}$$

is obtained (at Algorithm 1 lines 18, 21) as a function of ν_k, which works as a seed for the PDF computation. Finally, the new value ν_{k+1} is generated (at Algorithm 1 lines 22, 24), and coincides with the throughput achieved by $\boldsymbol{q}(\nu_k)$, i.e.

$$\nu_{k+1} = \Psi_{\boldsymbol{\alpha}}(\nu_k) \triangleq \rho_n\big(\boldsymbol{q}(\nu_k)\big). \tag{15}$$

Starting from ν_{k+1}, the updated PDF $\boldsymbol{q}(\nu_{k+1})$ is calculated in the next iteration of Algorithm 1.

Note that, by construction, $\Psi_{\boldsymbol{\alpha}}(\nu)$ is the *restriction* of throughput function (6) from the set of all feasible PDFs

$$\mathcal{Q} \triangleq \{\boldsymbol{q} \in [0,1]^{m+1} \mid \mathbf{1}^{\boldsymbol{T}}\boldsymbol{q} = 1\} \tag{16}$$

to the subset

$$\mathcal{Q}' \triangleq \{\boldsymbol{q}(\nu), \nu \in [0, \alpha_{\max}]\} \tag{17}$$

of PDFs generated by Algorithm 1 lines 6-21 for any given value of ν.

By inspection, it can be noticed that Algorithm 1 terminates when a fixed-point value ν^* of $\Psi_{\boldsymbol{\alpha}}(\cdot)$ is found[3]

$$\nu^* = \Psi_{\boldsymbol{\alpha}}(\nu^*)$$

Note that throughput (6) (and, consequently, the fixed-point function $\Psi_{\boldsymbol{\alpha}}(\cdot)$ in (15)) is bounded above by $\alpha_{\max}$. Thus, we can reduce ν domain to the interval $[0, \alpha_{\max}]$ (nonempty compact convex set). Therefore, by invoking Brouwer's fixed point theorem, it follows that there exists at least a fixed point ν^*. In Appendix A we prove the following result.

Theorem 2: The global optimum ρ_n^* of (6) is both a fixed point of $\Psi_{\boldsymbol{\alpha}}(\nu)$ and its maximum, i.e., any other $\nu \in [0, \alpha_{\max}]$, with $\nu \ne \rho_n^*$, generates a PDF $\boldsymbol{q}(\nu) \in \mathcal{Q}'$ whose throughput $\rho_n\big(\boldsymbol{q}(\nu)\big) \equiv \Psi_{\boldsymbol{\alpha}}(\nu)$ satisfies

$$\Psi_{\boldsymbol{\alpha}}(\nu) \le \Psi_{\boldsymbol{\alpha}}(\rho_n^*) = \rho_n^*. \tag{18}$$

Furthermore, the optimal PDF $\boldsymbol{q}^*$ belongs to the subset $\mathcal{Q}'$ in (17) and corresponds to the seed $\nu := \rho_n^*$, i.e., $\boldsymbol{q}^* \equiv \boldsymbol{q}(\rho_n^*)$. Then, in Appendix B we prove that the derived fixed-point system exactly admits one fixed point (i.e., the global optimum), and Algorithm 1 converges to it.

Remark: We explicitly stress that in Appendix A we led derivations assuming $\alpha_j > 0$ to be concise. In fact,

[3]Namely, when iteration (13) converges to a fixed point within the desired numerical accuracy ε.

Algorithm 1 Pseudo-Code of q_j's Computation ($\alpha_j \geq 0$)

$s \leftarrow 0/1$ (skip flag)
$\nu \leftarrow 0$
$E \leftarrow 1$
$\tau_m \leftarrow 1$
while $E > \epsilon$ **do**
  $j^+ \leftarrow m$
  $\sigma \leftarrow s \cdot \nu$
  for $j = m+s-1, \ldots, 1$ **do**
    $x_j \leftarrow \max\{0, \alpha_j + \nu\beta(j^+ - j) - \sigma\}/(n-1)$
    $\tau_j \overset{(\lim)}{\leftarrow} x_j/(\alpha_j + x_j)$
    if $x_j > 0$ **then**
      $j^+ \leftarrow j$
      $\sigma \overset{(\lim)}{\leftarrow} \alpha_{j^+}/(1 + x_{j^+}/\alpha_{j^+})^{n-1}$
    end if
  end for
  $F_0 \leftarrow 0$
  for $j = 1, \ldots, m$ **do**
    $q_j \leftarrow \tau_j(1 - F_{j-1})$
    $F_j \leftarrow q_j + F_{j-1}$
  end for
  $q_{m+1} \leftarrow 1 - F_m$
  $\rho_n \leftarrow \frac{n\sum_{i=1}^{m}\alpha_i q_i (1-F_i)^{n-1}}{1+\beta-q_{m+1}^n+\beta\sum_{i=1}^{m-1}(1-F_i)^n}$
  $E \leftarrow |\rho_n - \nu|/\rho_n$
  $\nu \leftarrow \rho_n$
end while

Equation (29) ceases to be useful (or even valid) when $\alpha_j = 0$. Nevertheless, one can prove that Algorithm 1 continue to achieve the optimal PDF under the more general condition $\alpha_j \geq 0$, so long as to consider the assignment statements in line 10 and line 13 of Algorithm 1 in the limit for the weight tending to 0, i.e.

$$10: \quad \tau_j \leftarrow 0, \qquad \text{if } \alpha_j = x_j = 0$$
$$13: \quad \sigma \leftarrow 0, \qquad \text{if } \alpha_{j^+} = 0$$

We use the symbol $\overset{(\lim)}{\leftarrow}$ in Algorithm 1 to emphasize this point.

In the remaining part of this section we restrict ourselves to the case of un-weighted throughput ($\alpha_j = 1, \forall j$). The computation of the dummy variables x_j, $j = 1, \ldots, m$, in this setting is simpler than in the general case. The full specialized algorithm, including the fixed point loop iteration, is presented in Algorithm 2.

We prove that, in case $s = 1$, the optimal PDF leads to a simple Geometric PDF for the backoff countdown. This result proves, for the first time to the best of our knowledge, that the typical assumption made in the analysis of non-persistent CSMA, ever since the seminal paper by Kleinrock and Tobagi [12], is actually *the best possible choice* under the respect of throughput.

Formally, we have the following statement (see Appendix C for its proof).

Theorem 3: The PDF of back-off that maximizes the un-weighted throughput in Equation (5) when skip is allowed is a Geometric distribution defined by $q_i = \tau(1-\tau)^{i-1}$, $i = 1, \ldots, m$, and $q_{m+1} = (1-\tau)^m$, where τ is the unique solution in $(0,1)$ of the equation

$$(1-\tau)^n = (1+\beta)(1-n\tau) \tag{19}$$

It is an intriguing result that the possibly simplest PDF of back-off is also the best possible choice as far as throughput is concerned and skip allowed. Moreover, the Geometric PDF dissipates the effect of the contention window size m, so that the optimized normalized throughput is independent of m. This property is consistent with the memoryless property of the Geometric PDF. This is also quite easy to implement, since it requires only one parameter, namely the unique solution τ^* of Equation (19). In general, τ^* is dependent on n. It can be verified numerically however that τ^* is weakly dependent on n, except for very small values of n. Its approximation to the leading term is expressed as $\tau^* \approx \xi/n$, where ξ is the unique solution of

$$e^{-x} = (1+\beta)(1-x), \qquad x \in [0,1] \tag{20}$$

It turns out that ξ/n provides an accurate approximation of τ^* for essentially all values of n and it is asymptotically sharp as $n \to \infty$.

Algorithm 2 Pseudo-Code of x_j's Computation ($\alpha_j = 1$)

$s \leftarrow 0/1$ (skip flag)
$\rho_n \leftarrow 0$
$E \leftarrow 1$
while $E > \epsilon$ **do**
  $x_{m+s-1} \leftarrow \frac{1}{n-1}\left[1 + \rho_n\beta - s\rho_n(1+\beta)\right]$
  for $j = m+s-2, \ldots, 1$ **do**
    $x_j \leftarrow \frac{1}{n-1}\left[1 + \rho_n\beta - \frac{1}{(1+x_{j+1})^{n-1}}\right]$
  end for
  $F_0 \leftarrow 0$
  for $j = 1, \ldots, m+s-1$ **do**
    $q_j \leftarrow \frac{x_j}{1+x_j}(1 - F_{j-1})$
    $F_j \leftarrow q_j + F_{j-1}$
  end for
  $q_{m+s} \leftarrow 1 - F_{m+s-1}$
  $\rho'_n \leftarrow \frac{n\sum_{i=1}^{m} q_i(1-F_i)^{n-1}}{1+\beta-q_{m+1}^n+\beta\sum_{i=1}^{m-1}(1-F_i)^n}$
  $E \leftarrow |\rho'_n - \rho_n|/\rho'_n$
  $\rho_n \leftarrow \rho'_n$
end while

V. Numerical Results

Numerical examples to assess properties of the optimal PDF of back-off and its impact on CSMA performance are given in Section V-A. A specific use case of the weighted throughput, in an energy constrained scenario, is then presented in Section V-B.

A. Optimal PDF Performance

Figure 2 shows the normalized throughput (i.e., channel utilization) as a function of the window size m, for different values of β and $\alpha_j = 1$, $j = 1, \ldots, m$). Two cases are shown: $n = 30$ STAs (upper plot), and $n = 90$ STAs (lower plot). We compare three back-off PDFs: *i)* optimal PDF strategy

with 'skip' possibility ($s = 1$) (curves labeled with s-PDF); *ii)* optimal PDF strategy without 'skip' possibility ($s = 0$) (curves labeled with $\overline{s}$-PDF); and *ii)* uniform distribution (curves labeled with u-PDF).

From Figure 2 we obtain some useful insights. First, as one can expect, s-PDF is the best performing, due to the additional 'skip' degree of freedom. Second, the smaller is β, the higher is the m value $\overline{s}$-PDF needs to achieve performance provided by s-PDF (to appreciate this fact, Figure 2(a) is in linear scale); however, the sensitivity is low and convergence is achieved within m of the order of 26 both in Figure 2(a) and Figure 2(b), emregardless of the value of n. Noticeably, we explicitly point out that optimal PDFs s-PDF and $\overline{s}$-PDF *equalize* the n-dependence, i.e., their performance slightly depend on n. This is compliant with a well-known property that characterizes optimized CSMA/CA systems [11], [20], [29]. Fourth, optimal PDFs significantly outperform uniform distribution strategies. This is particularly evident in Figure 2(b), where we show performance up to $m = 2048$ (logarithmic scale), for $n = 90$. Unlike $\overline{s}$-PDF, the u-PDF optimized contention window size m strongly depends on both β and n, and rapidly increases with the latter. This confirms the discussion in Section II about uniform distribution sensitivity to system parameters and the need of adaptation algorithms to properly set m. In fact, this is a (still open) issue, being adaptation algorithms notoriously short-term unfair and with long transients. They are a major bottleneck in random access, especially for massive scenarios. To provide an example, the optimized m value spans from around 64 for $\beta = 1/10$, $n = 30$ (beyond the range depicted in Figure 2(a)) to more than 512 for $\beta = 1/100$, $n = 90$ (Figure 2(b))), and rapidly become unpractical in massive high-density scenarios, or whenever an application-dependent constraint on m must be considered (for instant, latency constraints for event-driven and/or safety services).

Finally, noticeably, s-PDF's throughput is independent of m. This is confirmed by Figure 3, showing fixed-point function $\rho_{\text{out}} = \Psi(\rho_{\text{in}})$ of Algorithm 1 and its intersection with the bisector (namely, the fixed-points related to PDFs stable optimized performance) for different values of m. For $s = 1$, there is a *common* fixed-point, regardless of m (Figure 3(a)), whereas, for $s = 0$, fixed-points converge to the optimal one provided by s-PDF for increasing values of m (Figure 3(b)).

Concerning sensitivity to starting setting ρ_{in}, curves in Figure 3(b) are approximately flat for any m, thus indicating $\overline{s}$-PDF is extremely robust with respect to the tentative value ρ_{in} used to initialize Algorithm 1. Conversely, s-PDF is more sensitive to ρ_{in} for relatively low values of m, despite its optimal point being independent of m (see Figure 3(a)). Hence, Figure 3 provides a trade-off among performance and sensitivity (equivalently, time needed to converge to the optimal distribution). Nevertheless, Table II indicates that computational complexity to converge to fixed-point is limited to just a few iterations of Algorithm 1, when $\rho_{\text{in}} = 0$ is used as starting point and 1e−8 and 1e−12 are set as numerical tolerance, respectively.

Moving to the case with non-uniform weights, we define three weight vectors $\boldsymbol{\alpha}^{(1)}$, $\boldsymbol{\alpha}^{(2)}$ and $\boldsymbol{\alpha}^{(3)}$, each of size $m = 36$. Their values are listed in Table III. The weight values can be interpreted as rewards for winning the contention upon a given back-off slot, and their setting is context and application dependent.[4] Note that $\boldsymbol{\alpha}^{(1)}$ corresponds to the baseline uniform

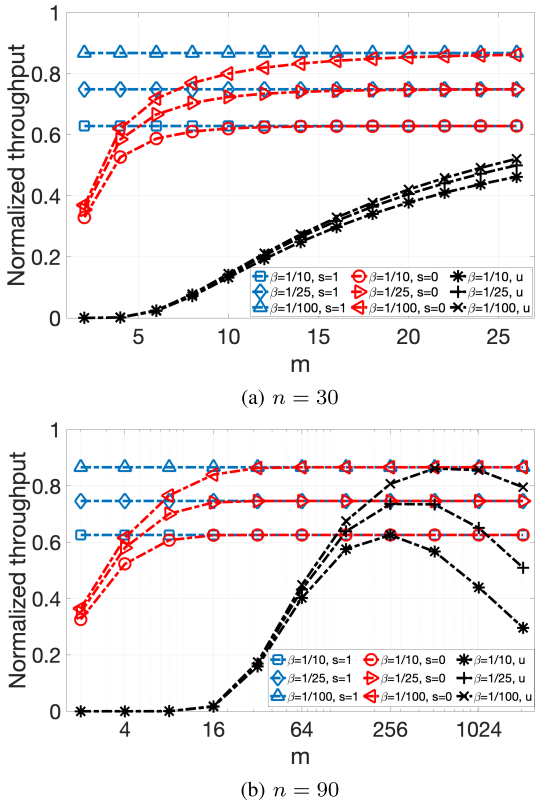

(a) $n = 30$

(b) $n = 90$

Fig. 2. Normalized throughput versus contention window size m. Comparison among optimal PDF without and with skip ($s = 0/1$) and a uniform PDF (u), in case of uniform weights ($\alpha_j = 1$, $j = 1, \ldots, m$), and various values of n and β.

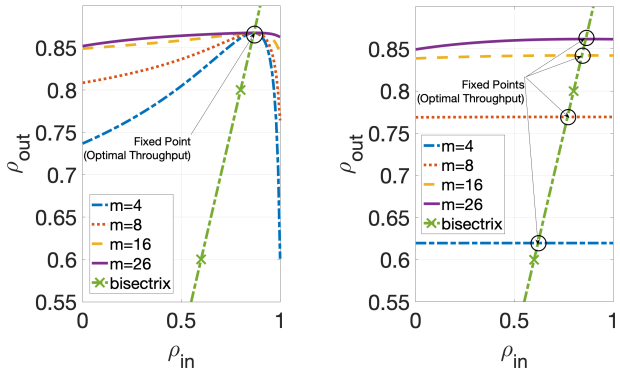

(a) Skip allowed ($s = 1$)

(b) Skip not allowed ($s = 0$)

Fig. 3. Fixed-point function $\rho_{\text{out}} = \Psi(\rho_{\text{in}})$ for: (a) $s = 1$, (b) $s = 0$, in case of uniform weights ($\alpha_j = 1$, $j = 1, \ldots, m$), $\beta = 1/100$, $n = 30$.

TABLE II

NUMBER OF ITERATIONS TO CONVERGE TO THE FIXED-POINT ($\beta = 1/100$, $n = 30$, $\rho_{\text{IN}} = 0$)

m	4	8	16	26
$s = 1$ (tol. 1e-8)	6	5	4	4
$s = 0$ (tol. 1e-8)	3	3	4	4

m	4	8	16	26
$s = 1$ (tol. 1e-12)	7	6	5	5
$s = 0$ (tol. 1e-12)	3	4	4	4

[4] A practical example is given in the following subsection.

TABLE III

WEIGHT VECTORS USED FOR THE NON-UNIFORM CASE. $\alpha^{(1)}$ CORRESPONDS TO THE BASELINE UNIFORM WEIGHTS CASE, WHILE $\alpha^{(2)}$ AND $\alpha^{(3)}$ ARE TWO BLOCK-TYPE CHANNEL-REWARDS

slot-index j	1–9	10-18	19-27	28-36
channel rewards $\boldsymbol{\alpha}^{(1)}$	1	1	1	1
channel rewards $\boldsymbol{\alpha}^{(2)}$	2.5	2	3	3.5
channel rewards $\boldsymbol{\alpha}^{(3)}$	1.5	2.5	3.5	3

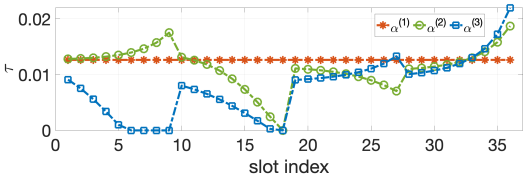

(a) Optimal PDF

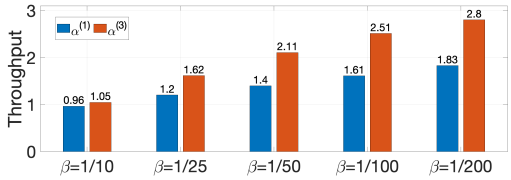

(b) Performance comparison

Fig. 4. (a) Conditional back-off probabilities τ_j with skip ($s = 1$) for the optimal back-off PDF as a function of m, with the three different set of weights shown in Table III, for $\beta = 1/10$ and $n = 30$. (b) Throughput related to metrics $\alpha^{(3)}$, achieved by the PDF optimized for channel utilization ($\alpha^{(1)}$ in the legend) and the PDF explicitly optimized for the considered scenario ($\alpha^{(3)}$ in the legend), for $m = 36$, $n = 30$.

weights case (i.e., channel utilization). From a theoretical point of view, we say that each weight vector characterizes a different MAC channel. For the considered weight vectors $\boldsymbol{\alpha}^{(1)}$, $\boldsymbol{\alpha}^{(2)}$ and $\boldsymbol{\alpha}^{(3)}$, Figure 4(a) plots the corresponding optimal conditional probabilities τ_j, $j = 1, \ldots, m$ (see Table I and Equation (11)) for $s = 1$ (skip allowed), as a function of j, for $1 \leq j \leq m$. Some valuable insights can be obtained by inspecting these curves. First, for $\boldsymbol{\alpha}^{(1)}$ (i.e., uniform case), we have: $\tau_1 = \tau_2 = \ldots = \tau_m = \tau$, i.e., the Geometric PDF *is* the optimal back-off distribution,[5] confirming the established theoretical results. Second, curves in Figure 4(a) show that the Geometric PDF is no longer optimal for the block-type channel rewards $\boldsymbol{\alpha}^{(2)}$ and $\boldsymbol{\alpha}^{(3)}$. Specifically, the optimized conditional access probability τ_i is in general a function of the *slot index* i.

Finally, to obtain some insights about performance gain offered by the PDF optimized for a considered MAC channel, Figure 4(b) shows, for different values of β, the weighted throughput when the channel is characterized by weights $\boldsymbol{\alpha}^{(3)}$. We compare the Geometric PDF (bars labeled with $\alpha^{(1)}$ in the figure), and the s-PDF explicitly optimized for the $\boldsymbol{\alpha}^{(3)}$ weights (bars labeled with $\alpha^{(3)}$ in the figure). More in dept, we compare the obtained average reward achieved by the 'general purpose' Geometric PDF maximizing channel utilization, and the PDF explicitly tuned for the considered reward scenario. Accordingly, in both cases the weighted throughput is measured using the rewards provided by the vector $\boldsymbol{\alpha}^{(3)}$, so that the Geometric PDF is actually mismatched. From Figure 4(b), optimal s-PDF's throughput gain over Geometric one spans from 9% to 53% in the considered β settings. Interestingly, Figure 4(b) shows that reducing β (i.e., increasing packet length, hence the packet transmission time T) is not sufficient to properly boost CSMA/CA performance, unless the optimal PDF is used. As an example, by decreasing β from $1/10$ to $1/200$ (i.e., a $20\times$ factor), Geometric throughput increase is limited to 91%, while the optimal one is 167%.

[5]We explicitly note that this is no longer the case when $s = 0$.

B. Energy Consumption Use Case

As an example of applicability of the weighted throughput in Equation (6) to a practical use case, in this subsection we tailor the weight vector $\boldsymbol{\alpha}$ to take account of STAs' energy consumption in a typical IoT setting, inspired to IEEE 802.11ah. In energy sensitive application scenarios, the target is not only to maximize network throughput, but also to minimize the consumed energy per successfully delivered packet. In this regards, Table IV lists the energy consumption of a STA in different modes, taken from [35] and [36]. Accordingly, for $i = 1, \ldots, m$, let

$$E_i^{(STA)} = (i-1)P_{RX}\delta + P_{TX}T \tag{21}$$

$$E_i^{(NET)} = n(i-1)P_{RX}\delta + (n-1)P_{RX}\delta + P_{TX}T + (n-1)P_{SL}(T-\delta). \tag{22}$$

the energies consumed within each Contention Cycle (CC). More in dept, Equation (21) is the energy consumed by a STA that wins the contention at slot i, whereas Equation (22) is the energy consumed by the whole network in case contention is won by a STA at slot i. To take into account energy consumption while maximizing throughput, we propose the following two weight settings, $\boldsymbol{\alpha}^{(STA)}$ and $\boldsymbol{\alpha}^{(NET)}$, so defined

$$\alpha_i^{(STA)} = 1/E_i^{(STA)}, \quad i = 1, \ldots, m \tag{23}$$

$$\alpha_i^{(NET)} = 1/E_i^{(NET)}, \quad i = 1, \ldots, m. \tag{24}$$

Roughly speaking, under framework (23) STAs are selfish-oriented, only considering their own consumed energy in throughput weighting, and always assume to be the winning STA while planning the PDF strategy. On the contrary, under framework (24) contention is network oriented, also accounting for sensing and sleeping energies of STAs that lose the contention. We compare the three settings $\boldsymbol{\alpha}^{(STA)}$, $\boldsymbol{\alpha}^{(NET)}$, $\boldsymbol{\alpha}^{(PHY)} = \mathbf{1}_m = [1, 1, , \ldots, 1]$, the last one corresponding to the PDF maximizing channel utilization (and, consequently, PHY throughput). Without ambiguity, with a slight abuse of notation, we refer to $\boldsymbol{\alpha}^{(STA)}$, $\boldsymbol{\alpha}^{(NET)}$, $\boldsymbol{\alpha}^{(PHY)}$ also to denote the corresponding PDF distributions. Table V lists network parameters used in simulations, which refer to IEEE 802.11ah technology [35]. Unless otherwise stated, each plotted point is an average over 10^5 CCs.

Figure 5 and Figure 6 show throughput and energy performance in basic access mode (no RTS/CTS), for $m = 64$ slots and $s = 0$ (no skip allowed), in terms of successfully transmitted Mbits/s (i.e., PHY throughput) and average consumed energy per successful packet transmission. For each PDF strategy, we test modulation and coding scheme 0 (MCS 0),

TABLE IV
POWER CONSUMPTION VALUES IN DIFFERENT MODES

mode	Power consumption (mW)
Transmission (P_{TX})	255
Receive and Channel Sensing (P_{RX})	135
Sleep (P_{SL})	1.5

TABLE V
USED IEEE 802.11AH BASIC ACCESS SYSTEM PARAMETERS

Definition	Value
Packet Payload	256 bytes
Symbol time, T_{sym}	40 μs
MAC header	14×8 bits
PHY header	$6 \times T_{sym}$
Length of ACK	0×8 bits (only PHY header)
Basic data rate (MCS 0)	650 kbps
256-QAM, CR = 3/4 (MCS 8)	7800 kbps
SlotTime (δ)	52 μs
SIFS	160 μs
DIFS	SIFS + 2 $\times$ SlotTime

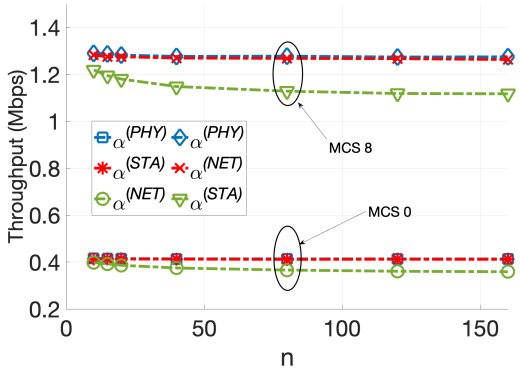

Fig. 5. Throughput achieved by PDFs $\boldsymbol{\alpha}^{(PHY)}$, $\boldsymbol{\alpha}^{(STA)}$ and $\boldsymbol{\alpha}^{(NET)}$ versus number of stations n, for $m = 64$, $s = 0$, MCS 0 and MCS 8.

corresponding to the basic data rate, and MCS 8, corresponding to 256-QAM (see Table V).

Some valuable insights can be obtained by the examination of these results. First, throughput performance of all PDFs are quite stable w.r.t. the number n of competing STAs, making them particularly attractive in application scenarios where a massive number of devices may compete for the channel in a short period of time, as a consequence of a triggering event (i.e., for massive machine type communication scenarios (mMTC)). Figure 5 shows that throughput only slightly decreases for increasing n. This is a consequence of the proposed optimal framework, which equalizes such a dependence. Second, $\boldsymbol{\alpha}^{(PHY)}$ achieves the best throughput performance, as expected. Nevertheless, $\boldsymbol{\alpha}^{(STA)}$ throughput is almost indistinguishable, whereas $\boldsymbol{\alpha}^{(NET)}$ PDF is only slightly less efficient.

Concerning energy efficiency, Figure 6 shows that both $\boldsymbol{\alpha}^{(STA)}$ and $\boldsymbol{\alpha}^{(NET)}$ outperform $\boldsymbol{\alpha}^{(PHY)}$. More in dept, the energy saving is particularly relevant for $\boldsymbol{\alpha}^{(NET)}$, and the slight reduction in its throughput performance (see Figure 5) is the price to pay for such an achievement in terms of energy efficiency. As an insightful example, $\boldsymbol{\alpha}^{(PHY)}$ consumes up to

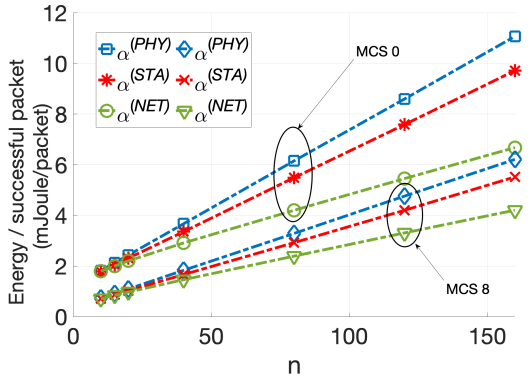

Fig. 6. Energy consumption of PDFs $\boldsymbol{\alpha}^{(PHY)}$, $\boldsymbol{\alpha}^{(STA)}$ and $\boldsymbol{\alpha}^{(NET)}$ versus number of stations n, for $m = 64$, $s = 0$, MCS 0 and MCS 8.

TABLE VI
COLLISION PROBABILITY (P_c), NUMBER OF CCS PER SUCCESSFUL PACKET TRANSMISSION (#CCS), AVERAGE NUMBER OF IDLE SLOTS PER CC (#ISS) ($n = 120$)

(MCS 0)	P_c	#CCs	#ISs	(MCS 8)	P_c	#CCs	#ISs
$\boldsymbol{\alpha}^{(PHY)}$	0.0721	1.0778	6.2187	$\boldsymbol{\alpha}^{(PHY)}$	0.1265	1.1448	3.2719
$\boldsymbol{\alpha}^{(STA)}$	0.0886	1.0972	4.9436	$\boldsymbol{\alpha}^{(STA)}$	0.1551	1.1836	2.5512
$\boldsymbol{\alpha}^{(NET)}$	0.2335	1.3047	1.4998	$\boldsymbol{\alpha}^{(NET)}$	0.2966	1.4216	1.0476

TABLE VII
u-PDF THROUGHPUT LOSS AND ENERGY LOSS (W.R.T. $\boldsymbol{\alpha}^{(PHY)}$ AND $\boldsymbol{\alpha}^{(NET)}$, RESPECTIVELY), FOR $m = 64$, MCS 0 AND IEEE 802.11AH PARAMETERS GIVEN IN TABLE IV

n	40	80	160
Throughput loss	17%	41%	73%
Energy loss	6%	38%	179%

65% (MCS 8, $n = 160$) and 48% (MCS 0, $n = 160$) more as compared to $\boldsymbol{\alpha}^{(NET)}$. Despite this, throughput loss of $\boldsymbol{\alpha}^{(NET)}$ in comparison with $\boldsymbol{\alpha}^{(PHY)}$ is limited up to 12% (both MCS 0 and MCS 8) (see Figure 5).

Table VI provides some additional metrics to explain the rationale behind differently optimized PDF strategies. Specifically, energy consumption critically depends on the non trivial trade-off between the number of contention cycles per successful packet transmission #CCs, and the average CC duration. As one can notice from Table VI, $\boldsymbol{\alpha}^{(STA)}$ and $\boldsymbol{\alpha}^{(NET)}$ are more aggressive compared to $\boldsymbol{\alpha}^{(PHY)}$, especially $\boldsymbol{\alpha}^{(NET)}$, resulting in an increased collision probability P_c, which negatively affects throughput and #CCs. Nevertheless, $\boldsymbol{\alpha}^{(STA)}$ and $\boldsymbol{\alpha}^{(NET)}$ strongly reduce the average number of idle slots #ISs per CC, and, consequently, the average CC duration. The optimized final trade-off is responsible for the energy gain in Figure 6.

Finally, from Figure 5 it can be recognized that throughput marginal loss of $\boldsymbol{\alpha}^{(NET)}$ rapidly stabilizes for increasing n (i.e., the $\boldsymbol{\alpha}^{(NET)}$ curves are approximately flat for high values of n), while the energy saving is more and more relevant as network size increases, which makes the use of the derived energy-oriented PDFs particularly advantageous in massive scenarios. To conclude, for the considered system parameters and MCS 0, Table VII provides the uniform

distribution (u-PDF) throughput reduction w.r.t the throughput benchmark provided by $\boldsymbol{\alpha}^{(PHY)}$ (throughput loss), and the energy consumption increase per successfully delivered packet w.r.t. the energy benchmark provided by $\boldsymbol{\alpha}^{(NET)}$ (energy loss), respectively.

VI. Conclusion

A major component of multiple access system, namely the CSMA protocol, is addressed and saturation throughput optimization is investigated. The special perspective of this work consists of assuming as degree of freedom in the optimization process the probability distribution of the back-off countdown, given the maximum size m of the contention window. The baseline CSMA, as presented in analytical works and as implemented in WiFi, adopts consistently a Geometric (memoryless) distribution of back-off or a uniform probability distribution over a variable contention window size, due to binary exponential back-off. The aim of this paper is investigating the opportunity offered by an alternative approach to CSMA throughput optimization.

To this end, a generalized notion of weighted throughput is introduced, which encompasses the traditional saturation throughput as a special case. Then, we present two major results. The optimal PDF of back-off in the general case of arbitrary non-negative weights is determined, providing a numerical algorithm for its construction. Moreover, in the particular case of weights all equal to 1, we have proved that the optimal PDF of back-off reduces to a Geometric distribution when contention window skip is allowed, thus unveiling an interesting property of this popular probability distribution of back-off, often simply justified in previous works for easiness of analysis. Here it is formally proved that it is actually the best possible choice, as far as saturation throughput is concerned.

Further work in the direction of this paper can be developed following two lines. On a practical side, distributed and adaptive algorithms for adjusting the probability distribution of back-off of a set of stations should be defined, to turn the result presented in this paper into an operative algorithm in a CSMA network where the number of contending stations varies over time. From a modeling point of view, more general optimization problems could be considered, involving multi-objectives, beside saturation throughput, e.g., time deadlines, or using utility functions to take traffic importance into account.

Appendix A
The Optimal Throughput as a Solution of the Fixed Point System in Algorithm 1

In this appendix we prove that the fixed point system in Algorithm 1 derives from a one-to-one manipulation (i.e., the pair-wise difference) of partial derivatives of the weighted throughput objective function, and corresponds to the study of their sign within the feasible region, in search of relative maxima.

The countdown PDF is given by a row vector $\mathbf{q} = [q_1, \ldots, q_{m+1}]$ of size $m+1$. We first consider the case $s = 1$. Since the sum of the components of the probability vector $\mathbf{q}$ must be 1, we have m independent variables, composing the vector $\mathbf{q}' = [q_1, \ldots, q_m]$, with the constraint that $q_i \geq 0$, $i = 1, \ldots, m$ and $q_1 + \cdots + q_m \leq 1$. We can re-write the weighted throughput in the following way, so that only the probabilities in $\mathbf{q}'$ are involved:

$$\rho_n^{(\boldsymbol{\alpha})} = \frac{n \sum_{j=1}^{m} \alpha_j q_j (1-F_j)^{n-1}}{1 + \beta - (1-F_m)^n + \beta \sum_{j=1}^{m-1} (1-F_j)^n}. \tag{25}$$

In this appendix, we omit the $(\boldsymbol{\alpha})$ superscript in throughput notation without any ambiguity. We regard ρ_n as a function of $\mathbf{q}'$ and let

$$\rho_n = \frac{P_s^{(\boldsymbol{\alpha})}(\mathbf{q}')}{D(\mathbf{q}')} \tag{26}$$

where

$$P_s^{(\boldsymbol{\alpha})}(\mathbf{q}') = n \sum_{j=1}^{m} \alpha_j q_j (1-F_j)^{n-1} \tag{27}$$

and

$$D(\mathbf{q}') = 1 + \beta - (1-F_m)^n + \beta \sum_{i=1}^{m-1} (1-F_i)^n. \tag{28}$$

We lead derivations assuming $\alpha_j > 0$ in this section, to be concise. We now derive an algorithm producing the optimal PDF $\mathbf{q}'$ in terms of the related auxiliary variables

$$x_j \triangleq \frac{\alpha_j q_j}{1 - F_j} \tag{29}$$

for $j = 1, \ldots, m$, with $x_j \in [0, +\infty[$. Hence, once the optimal x_j are computed, from (29) and τ_j's definition (11) we obtain probabilities τ_j and q_j as

$$\tau_j = \frac{x_j}{\alpha_j + x_j} \tag{30}$$

for $j = 1, \ldots, m$, and

$$q_j = \tau_j \cdot (1 - F_{j-1}). \tag{31}$$

for $j = 1, \ldots, m+1$, being, by position, $\tau_{m+1} = 1$.[6]

Recursion Equation (31) can be solved, yielding

$$q_j = \begin{cases} \dfrac{x_1}{\alpha_1 + x_1} & j = 1 \\ \dfrac{x_j}{\alpha_j + x_j} \displaystyle\prod_{k=1}^{j-1} \frac{\alpha_k}{\alpha_k + x_k} & j = 2, \ldots, m \\ 1 - \displaystyle\sum_{j=1}^{m} q_j & j = m+1 \end{cases} \tag{32}$$

To maximize ρ_n in (25), we study the sign of its partial derivatives, which are

$$\begin{aligned} \frac{\partial \rho_n}{\partial q_j} &= \frac{1}{D(\mathbf{q}')} \left[\frac{\partial P_s^{(\alpha)}}{\partial q_j} - \frac{P_s^{(\alpha)}}{D(\mathbf{q}')} \frac{\partial D}{\partial q_j} \right] \\ &= \frac{1}{D(\mathbf{q}')} \left[\frac{\partial P_s^{(\alpha)}}{\partial q_j} - \rho_n \frac{\partial D}{\partial q_j} \right] = \frac{n N_j(\mathbf{q}')}{D(\mathbf{q}')} \end{aligned} \tag{33}$$

[6] $\tau_{m+1} = 1$ accounts for the constraint $q_{m+1} = 1 - (q_1 + \cdots + q_m)$. Note that for $\alpha_j > 0$ Equation (29) is always well defined. Furthermore, $x_j = 0$ iff $q_j = 0$.

where

$$N_j(\mathbf{q}') = \alpha_j (1-F_j)^{n-1} - (n-1)\sum_{i=j}^{m} \alpha_i q_i (1-F_i)^{n-2} + \rho_n \beta \sum_{i=j}^{m-1} (1-F_i)^{n-1} - \rho_n (1-F_m)^{n-1} \quad (34)$$

for $j = 1, \ldots, m$. Note that, for any feasible $\mathbf{q}'$, we have $D(\mathbf{q}') > 0$. As a consequence, the sign of (33) only depends on the sign of $N_j(\mathbf{q}')$. We proceed backwards in the study of it, for $j = m, \ldots, 1$.

Base case ($j = m$): (34) simplifies to

$$N_m(\mathbf{q}') = \alpha_m (1-F_m)^{n-1} - (n-1)\alpha_m q_m (1-F_m)^{n-2} - \rho_n (1-F_m)^{n-1}. \quad (35)$$

By studying its sign, i.e., by solving the inequality $N_m(\mathbf{q}') \geq 0$, we get the following inequality

$$x_m \leq \frac{\alpha_m - \rho_n}{n-1} \quad (36)$$

where we used the position (29). Therefore, at the optimal point we have the following two possibilities: *i)* $\rho_n > \alpha_m$: in this case (36) is never satisfied, $N_m(\mathbf{q}')$ is always negative and ρ_n is a decreasing function of x_m, resulting in the optimal value $x_m = 0$ and, consequently, $\tau_m = 0$ and $q_m = 0$; *ii)* $\rho_n \leq \alpha_m$: in order for ρ_n to be a maximum it has to be, strictly, $x_m = (\alpha_m - \rho_n)/(n-1)$, which results in $N_m(\mathbf{q}') = 0$ and (see (33)) $\partial \rho_n(\mathbf{q}')/\partial q_m = 0$. Thus, in a compact notation, at the optimum we have[7]

$$x_m = \left[\frac{\alpha_m - \rho_n}{n-1}\right]_+ \quad (37)$$

and

$$\partial \rho_n(\mathbf{q}')/\partial q_m = 0 \quad \text{if } x_m > 0. \quad (38)$$

In the following, we use (38) as base case ($j = m$) to inductively proof backward such a result for any $j = m-1, \ldots, 1$.

Inductive step ($j < m$): let

$$\mathcal{I}_j^+ \triangleq \{ i \in \{j+1, \ldots, m\} \,|\, x_i > 0 \}. \quad (39)$$

By induction hypothesis, we have

$$\partial \rho_n(\mathbf{q}')/\partial q_i = 0, \quad \text{for any } i \in \mathcal{I}_j^+. \quad (40)$$

For the given j, there are two possibilities:

i) $\mathcal{I}_j^+ = \emptyset$. In such a case, since $q_i = 0$ for any $i > j$, (34) simplifies to

$$N_j(\mathbf{q}') = \alpha_j (1-F_j)^{n-1} - (n-1)\alpha_j q_j (1-F_j)^{n-2} + \rho_n \beta (m-j)(1-F_j)^{n-1} - \rho_n (1-F_j)^{n-1}. \quad (41)$$

Similarly to what done above for $N_m(\mathbf{q}')$, by studying its sign, at the optimal point we get

$$x_j = \left[\frac{\alpha_j + \rho_n \beta (m-j) - \rho_n}{n-1}\right]_+. \quad (42)$$

with $N_j(\mathbf{q}') = 0$ if $x_j > 0$, i.e., (40) is satisfied also for $i = j$, i.e., for $i \in \{j\} \cup \mathcal{I}_j^+$ and the induction is complete.

[7]By definition $[a]_+ \triangleq \max\{a, 0\}$.

ii) $\mathcal{I}_j^+ \neq \emptyset$. Let $j^+ \triangleq \min\{i | i \in \mathcal{I}_j^+\}$, i.e., let $j^+ > j$ be the slot index closest to j such that $x_{j^+} > 0$. For all the intermediate indices $i \in \{j+1, \ldots, j^+ - 1\}$ (possibly, an empty set of indices, in case $j^+ = j+1$), we have $q_i = 0$. By leveraging the induction hypothesis (40) (applied to $i = j^+$) we have $N_{j^+}(\mathbf{q}') = 0$. Studying the sign of $\partial \rho_n(\mathbf{q}')/\partial q_j$, namely, the inequality $N_j(\mathbf{q}') \geq 0$, is therefore equivalent, in this case, to $N_{j^+}(\mathbf{q}') - N_j(\mathbf{q}') \leq 0$, i.e., the difference of eq. (34) for the values j^+ and j, which provides the inequality

$$\alpha_{j^+} \left(1-F_{j^+}\right)^{n-1} - \alpha_j (1-F_j)^{n-1} + (n-1)\alpha_j q_j (1-F_j)^{n-2} - \rho_n \beta (j^+ - j)(1-F_j)^{n-1} \leq 0. \quad (43)$$

Re-arranging we get

$$\alpha_{j^+} \left(\frac{1-F_{j^+}}{1-F_j}\right)^{n-1} + (n-1)\frac{\alpha_j q_j}{1-F_j} \leq \alpha_j + \rho_n \beta (j^+ - j) \quad (44)$$

from which, by leveraging position (29), we get at the optimum

$$x_j = \frac{1}{n-1}\left[\alpha_j + \rho_n \beta (j^+ - j) - \frac{\alpha_{j^+}}{(1 + x_{j^+}/\alpha_{j^+})^{n-1}}\right]_+. \quad (45)$$

with $N_j(\mathbf{q}') = 0$ if $x_j > 0$, which, similarly to what done above, confirms validity of the (40) for $i = j < j^+$, i.e., for $i \in \{j\} \cup \mathcal{I}_j^+$, completing the proof of the inductive step.

For $s = 0$, the obtained results still hold, unless minor changes. The countdown PDF is given by the row vector $\mathbf{q} = [q_1, \ldots, q_{m+1}]$ with the constraint $q_{m+1} = 0$. The sum of its components must be 1. Thus, we have $q_m = 1 - F_{m-1}$, i.e. $F_m = 1$, and $m-1$ independent variables, composing the vector $\mathbf{q}' = [q_1, \ldots, q_{m-1}]$, with the constraint that $q_i \geq 0$, $i = 1, \ldots, m-1$ and $q_1 + \cdots + q_{m-1} \leq 1$. The weighted throughput in (25) reduces to

$$\rho_n = \frac{n \sum_{j=1}^{m-1} \alpha_j q_j (1-F_j)^{n-1}}{1 + \beta + \beta \sum_{j=1}^{m-1} (1-F_j)^n}. \quad (46)$$

By studying the sign of the partial derivatives of ρ_n, we derive the optimal working points x_j, $j = 1, \ldots, m-1$. For $\mathcal{I}_j^+ = \emptyset$ Equation (42) changes to

$$x_j = \left[\frac{\alpha_j + \rho_n \beta (m-j)}{n-1}\right]_+ \quad (47)$$

while, for $\mathcal{I}_j^+ \neq \emptyset$, Equation (45) still holds. Probability expressions (30) and (31) apply for $i = 1, \ldots, m-1$ and $i = 1, \ldots, m$, respectively, with the additional position $\tau_m = 1$ taking account of the constraint $F_m = 1$.

Algorithm 1 includes the above derived equations and both frameworks ($s = 1$ and $s = 0$) in a single formulation. It also includes the slightly more general setting $\boldsymbol{\alpha} \in (\mathbb{R}_0^+)^m - \{\mathbf{0}_m\}$, that can be derived as a limit case.

As a conclusion, eqs. (25), (30), (31), (45), and (42) (for $s = 1$) or (47) (for $s = 0$) define a fixed-point non-linear system of the form $\rho_n = \Psi_{\boldsymbol{\alpha}}(\rho_n)$, that the optimal throughput

ρ_n^* has to satisfy, and $\boldsymbol{q}(\rho_n^*) \in \mathcal{Q}'$ in (17) is the related optimal PDF, obtained for the setting $\nu := \rho_n^*$. More in dept, the generic iteration of Algorithm 1 (lines 6–24) is a function $\Psi_{\boldsymbol{\alpha}}(\nu)$ mapping the input parameter ν (lines 7 and 9) into the conditioned PDF $\boldsymbol{\tau}(\nu)$ (and $\boldsymbol{q}(\nu)$) (lines 10, 18 and 21), and its achieved throughput (line 22)

$$\Psi_{\boldsymbol{\alpha}}(\nu) \triangleq \rho_n\big(\boldsymbol{q}(\nu)\big). \tag{48}$$

We refer to $\Psi_{\boldsymbol{\alpha}}(\nu)$ as fixed point function, and it can be verified that is a continuous function. $\Psi_{\boldsymbol{\alpha}}(\nu)$ in (48) is, by construction, as the restriction of the weighted throughput function (25) to the set (17) of PDFs produced by Algorithm 1 (lines 6–24) for any given seed $\nu \in [0, \alpha_{\max}]$. Theorem 2 is therefore proved.

Appendix B
Uniqueness of the Fixed Point and Convergence of Algorithm 1 to It

We omit the n subscript in throughput notation without any ambiguity. For $\boldsymbol{\alpha} \in (\mathbb{R}_0^+)^m - \{\boldsymbol{0}_m\}$ and $\boldsymbol{\tau} \in [0,1]^m$, (25) can be rewritten as a function of the conditioned probabilities $\boldsymbol{\tau}$ as

$$\rho \equiv \rho^{(\boldsymbol{\alpha})}(\boldsymbol{\tau}) = P_s^{(\boldsymbol{\alpha})}(\boldsymbol{\tau})/D(\boldsymbol{\tau}) \tag{49}$$

where

$$P_s^{(\boldsymbol{\alpha})}(\boldsymbol{\tau}) = n \sum_{j=1}^{m} \frac{\alpha_j \tau_j}{1-\tau_j} \prod_{h=1}^{j} (1-\tau_h)^n \tag{50}$$

$$D(\boldsymbol{\tau}) = 1 + \beta - \prod_{h=1}^{m} (1-\tau_h)^n + \beta \sum_{j=1}^{m-1} \prod_{h=1}^{j} (1-\tau_h)^n. \tag{51}$$

(49) is a continuous and differentiable function of both $\boldsymbol{\alpha}$ and $\boldsymbol{\tau}$ and, for a given $\boldsymbol{\alpha}$, is a bounded function of $\boldsymbol{\tau}$ in the compact subset $[0,1]^m$ of $\mathbb{R}^m$. It follows that it has a global maximum in this subset, denoted by ρ^*.

From (49) and the one-to-one mapping (30) (i.e., Algorithm 1 line 10), the fixed point function can written as $\Psi_{\boldsymbol{\alpha}}(\nu) \equiv \rho\big(\boldsymbol{\tau}(\boldsymbol{x}(\nu))\big)$, where (see Algorithm 1, line 9)

$$x_j(\nu) = \max\{0, y_j(\nu)\} \tag{52}$$

with

$$y_j(\nu) \triangleq \frac{1}{n-1}\big(\alpha_j + \nu\beta(j^+ - j) - \sigma_j(\nu)\big). \tag{53}$$

By rearranging the partial derivative $\partial\rho(\boldsymbol{\tau})/\partial\tau_j$ similarly to what we did in (33), $\boldsymbol{\tau}(\nu)$ satisfies, by Algorithm 1 construction, the following equation

$$\frac{\partial P_s^{(\alpha)}(\boldsymbol{\tau}(\nu))}{\partial \tau_j} - \nu \frac{\partial D(\boldsymbol{\tau}(\nu))}{\partial \tau_j} = 0 \tag{54}$$

for a given ν, if $y_j(\nu) \geq 0$. Vice versa, if $y_j(\nu) < 0$, we have $\partial x_j(\nu)/\partial\nu = 0$. For the fixed point function derivative, we get[8]

$$\Psi'_{\boldsymbol{\alpha}}(\nu) = \sum_{j=1}^{m} \frac{\partial\rho}{\partial\tau_j}\frac{\partial\tau_j}{\partial x_j}\frac{\partial x_j}{\partial\nu}$$

$$= \sum_{j\in\mathcal{I}_+(\nu)} \frac{1}{D}\left[\frac{\partial P_s^{(\alpha)}}{\partial\tau_j} - \Psi_{\boldsymbol{\alpha}}(\nu)\frac{\partial D}{\partial\tau_j}\right]\frac{\alpha_j}{(\alpha_j + x_j)^2}\frac{\partial x_j}{\partial\nu} \tag{55}$$

where

$$\mathcal{I}_+(\nu) \triangleq \big\{j \in \{1,\dots,m\} \,|\, y_j(\nu) \geq 0\big\}. \tag{56}$$

By substituting expression (54) in the derivative (55), we get

$$\Psi'_{\boldsymbol{\alpha}}(\nu) = \big(\nu - \Psi_{\boldsymbol{\alpha}}(\nu)\big) g_{\boldsymbol{\alpha}}(\nu) \tag{57}$$

where

$$g_{\boldsymbol{\alpha}}(\nu) \triangleq \frac{1}{D(\boldsymbol{\tau}(\nu))} \sum_{j\in\mathcal{I}_+(\nu)} \frac{\partial D(\boldsymbol{\tau}(\nu))}{\partial\tau_j} \frac{\alpha_j}{(\alpha_j + x_i(\nu))^2}\frac{\partial x_j(\nu)}{\partial\nu}. \tag{58}$$

Note that, due to the max operator in (52), which takes into account the implicit box constraint $\boldsymbol{\tau} \in [0,1]^m$, left and right derivative of $x_j(\nu)$ in (58) assume finite values but may differ. Formally, let $\mathcal{I}_0(\nu) \triangleq \{j \in \{1,\dots,m\} | y_j(\nu) = 0\}\}$, and

$$\mathcal{S} \triangleq \{\nu \in [0, \alpha_{max}] \mid \mathcal{I}_0(\nu) \neq \emptyset\}. \tag{59}$$

For $\nu \notin \mathcal{S}$ the derivative is well defined, while for $\nu \in \mathcal{S}$ we may have $g_{\boldsymbol{\alpha}}(\nu^-) \neq g_{\boldsymbol{\alpha}}(\nu^+)$ due to the angular points in (52). Nevertheless, by leveraging the above detailed analysis, the following final results stem:

Theorem 4: The fixed point function $\Psi_{\boldsymbol{\alpha}}(\nu)$ has a unique fixed point.

Proof: Let ν_1 and ν_2 two fixed points, with $\nu_1 \neq \nu_2$. Let $\nu_1 < \nu_2$. From (57) we have $\Psi'_{\boldsymbol{\alpha}}(\nu_1) = \Psi'_{\boldsymbol{\alpha}}(\nu_2) = 0$. As a consequence, there exists a right interval of ν_1 where $\Psi_{\boldsymbol{\alpha}}(\nu)$ is below the bisector, and a left interval of ν_2 where $\Psi_{\boldsymbol{\alpha}}(\nu)$ is above the bisector. From continuity of $\Psi_{\boldsymbol{\alpha}}(\nu)$ in $[0, \alpha_{\max}]$, there exists $\overline{\nu} \in]\nu_1, \nu_2[$ where $\Psi_{\boldsymbol{\alpha}}(\nu)$ intersects the bisector, i.e., $\Psi_{\boldsymbol{\alpha}}(\overline{\nu}) = \overline{\nu}$, with $\Psi'_{\boldsymbol{\alpha}}(\overline{\nu}) \neq 0$ (more in dept, $\Psi'_{\boldsymbol{\alpha}}(\overline{\nu}) > 1$), contradicting (57). □

By leveraging Theorem 4 and Theorem 2, we conclude that there is a unique fixed-point ρ^*, which is also the unique global maximum of both (6) and its restriction $\Psi_{\boldsymbol{\alpha}}(\nu)$. i.e.,

$$\begin{cases} \Psi_{\boldsymbol{\alpha}}(\rho^*) = \rho^* \\ \Psi_{\boldsymbol{\alpha}}(\nu) < \rho^*, \quad \nu \in [0, \alpha_{\max}],\ \nu \neq \rho^*. \end{cases} \tag{60}$$

We can now prove the following final result.

Theorem 5: Algorithm 1 converges to $\Psi_{\boldsymbol{\alpha}}(\nu)$'s fixed point.

Proof: Let ρ^* be $\Psi_{\boldsymbol{\alpha}}(\cdot)$'s fixed point. By Algorithm 1 inspection it can be verified that $\Psi_{\boldsymbol{\alpha}}(0) > 0$.[9] Assume, by contradiction, that there exists $\overline{\nu} \in]0, \rho^*[$ such that $\overline{\nu} \geq \Psi_{\boldsymbol{\alpha}}(\overline{\nu})$. From the uniqueness of fixed-point it must be, strictly, $\overline{\nu} > \Psi_{\boldsymbol{\alpha}}(\overline{\nu})$. Let $\Phi_{\boldsymbol{\alpha}}(\nu) \triangleq \Psi_{\boldsymbol{\alpha}}(\nu) - \nu$. We have $\Phi_{\boldsymbol{\alpha}}(0) > 0$ and $\Phi_{\boldsymbol{\alpha}}(\overline{\nu}) < 0$. Consequently, for the intermediate values theorem, there exists $\widetilde{\nu} \in]0, \overline{\nu}[$ such that $\Phi_{\boldsymbol{\alpha}}(\widetilde{\nu}) = 0$, i.e., $\Psi_{\boldsymbol{\alpha}}(\cdot)$ would have a second fixed point $\widetilde{\nu} < \rho^*$, obtaining a contradiction. Thus, from the above analysis and (60) we have

$$\nu < \Psi_{\boldsymbol{\alpha}}(\nu) < \rho^*, \quad \text{for any } \nu < \rho^*. \tag{61}$$

[8]We omit the functional dependence of terms on ν to simplify notation.

[9]The results also follows from the uniqueness of the fixed-point ρ^*. If $\Psi_{\boldsymbol{\alpha}}(0) = 0$, $\nu = 0$ would be a second fixed-point, obtaining a contradiction.

As a consequence, iteration (13) leads to a monotonic increasing sequence $\{\nu_k\}_{k\geq 0}$ buonded above, which converges to ρ^*. Finally, Algorithm 1 also converges for any $\nu_0 \in [0, \alpha_{\max}]$. In fact, whether $\nu_0 \in]\rho^*, \alpha_{\max}]$, from (60) we have $\nu_1 = \Psi_{\boldsymbol{\alpha}}(\nu_0) < \rho^*$. Consequently, from (61) we conclude that the sequence $\{\nu_k\}_{k\geq 1}$ monotonically converges to ρ^*. □

APPENDIX C
CONCATENATED WEIGHTED THROUGHPUT PROBLEM ($s = 1$)

Theorem 3 is a straightforward consequence of a more general result standing for any given vector of weight values $\boldsymbol{\alpha} \in (\mathbb{R}_0^+)^m - \{\mathbf{0}_m\}$, then applied to the standard normalized throughput (i.e., channel utilization) as a special case. For the given m and $\boldsymbol{\alpha}$, let $k \in \mathbb{N}$ be any positive integer, and assume $k = 2$ for the sake of simplicity. Consider the weighted throughput function $\rho^{(\boldsymbol{\alpha'})}(\boldsymbol{\tau'}) \equiv \rho^{(\boldsymbol{\alpha},\boldsymbol{\alpha})}(\boldsymbol{\tau}_1, \boldsymbol{\tau}_2)$, over a doubled contention window size $m' \triangleq 2m$, with weight vector $\boldsymbol{\alpha'} \triangleq [\boldsymbol{\alpha}, \boldsymbol{\alpha}] \in (\mathbb{R}_0^+)^{m'} - \{\mathbf{0}_{m'}\}$, given by the repetition of $\boldsymbol{\alpha}$ over the slots $i \in \{m+1, \ldots, 2m\}$, i.e., $\alpha_i = \alpha_{i+m}$, for $i = 1, \ldots, m$, and $\boldsymbol{\tau'} \triangleq [\boldsymbol{\tau}_1, \boldsymbol{\tau}_2] \in [0,1]^{m'}$, with $\boldsymbol{\tau}_1, \boldsymbol{\tau}_2 \in [0,1]^m$. We refer to the here defined 2-dimensional weighted throughput as 2-fold concatenated throughput.[10] By rearranging terms in (49)–(51) we can write

$$\begin{aligned}\rho^{(\boldsymbol{\alpha},\boldsymbol{\alpha})}(\boldsymbol{\tau}_1, \boldsymbol{\tau}_2) &= \frac{P_s^{(\boldsymbol{\alpha})}(\boldsymbol{\tau}_1) + P_I(\boldsymbol{\tau}_1) P_s^{(\boldsymbol{\alpha})}(\boldsymbol{\tau}_2)}{D(\boldsymbol{\tau}_1) + P_I(\boldsymbol{\tau}_1) D(\boldsymbol{\tau}_2)} \\ &= \frac{D(\boldsymbol{\tau}_1)}{D(\boldsymbol{\tau}_1) + P_I(\boldsymbol{\tau}_1) D(\boldsymbol{\tau}_2)} \rho^{(\boldsymbol{\alpha})}(\boldsymbol{\tau}_1) \\ &\quad + \frac{P_I(\boldsymbol{\tau}_1) D(\boldsymbol{\tau}_2)}{D(\boldsymbol{\tau}_1) + P_I(\boldsymbol{\tau}_1) D(\boldsymbol{\tau}_2)} \rho^{(\boldsymbol{\alpha})}(\boldsymbol{\tau}_2) \quad (62)\end{aligned}$$

with $P_I(\boldsymbol{\tau}_1) \triangleq \prod_{h=1}^{m} (1 - \tau_h)^n$. Let $\boldsymbol{\tau}^* \in [0,1]^m$ be the global optimum of $\rho^{(\boldsymbol{\alpha})}(\boldsymbol{\tau})$, i.e., the base maximization problem over m slots, for the given $\boldsymbol{\alpha}$. From (62) we conclude that $\boldsymbol{\tau'}^* \triangleq [\boldsymbol{\tau}^*, \boldsymbol{\tau}^*] \in [0,1]^{2m}$ is the global optimum of the concatenated throughput $\rho^{(\boldsymbol{\alpha},\boldsymbol{\alpha})}(\boldsymbol{\tau}_1, \boldsymbol{\tau}_2)$, with $\rho^{(\boldsymbol{\alpha},\boldsymbol{\alpha})}(\boldsymbol{\tau}^*, \boldsymbol{\tau}^*) = \rho^{(\boldsymbol{\alpha})}(\boldsymbol{\tau}^*)$.

Theorem 3 follows as a direct application of this result to the normalized throughput, which can be considered as the m-fold concatenated problem of the base case $m = 1$, $\alpha = 1$. Eq. (19) directly follows from the study of the derivative of (7).

REFERENCES

[1] Y. C. Tay, K. Jamieson, and H. Balakrishnan, "Collision-minimizing CSMA and its applications to wireless sensor networks," *IEEE J. Sel. Areas Commun.*, vol. 22, no. 6, pp. 1048–1057, Aug. 2004.

[2] M. V. Bueno-Delgado, R. Ferrero, F. Gandino, P. Pavon-Marino, and M. Rebaudengo, "A geometric distribution reader anti-collision protocol for RFID dense reader environments," *IEEE Trans. Autom. Sci. Eng.*, vol. 10, no. 2, pp. 296–306, Apr. 2013.

[3] P. K. Sahoo and J.-P. Sheu, "Design and analysis of collision free MAC for wireless sensor networks with or without data retransmission," *J. Netw. Comput. Appl.*, vol. 80, pp. 10–21, Feb. 2017.

[4] C. García-Costa, E. Egea-López, and J. García-Haro, "Evaluation of MAC contention techniques for efficient geo-routing in vehicular networks," *Ad Hoc Netw.*, vol. 37, pp. 44–62, Feb. 2016.

[10] The proof detailed in this appendix holds for any k, with obvious changes to derive the k-fold concatenated throughput. We assume $k = 2$ for the sake of brevity and avoid cumbersome notation.

[5] E. Khorov et al., "Enabling the Internet of Things with Wi-Fi halow—Performance evaluation of the restricted access window," *IEEE Access*, vol. 7, pp. 127402–127415, 2019.

[6] Y. Cheng, D. Yang, H. Zhou, and H. Wang, "Adopting IEEE 802.11 MAC for industrial delay-sensitive wireless control and monitoring applications: A survey," *Comput. Netw.*, vol. 157, pp. 41–67, Jul. 2019.

[7] I. Demirkol and C. Ersoy, "Energy and delay optimized contention for wireless sensor networks," *Comput. Netw.*, vol. 53, no. 12, pp. 2106–2119, Aug. 2009.

[8] K. Jamieson, H. Balakrishnan, and Y. C. Tay, "Sift: A MAC protocol for event-driven wireless sensor networks," in *Wireless Sensor Networks*, K. Römer, H. Karl, and F. Mattern, Eds. Berlin, Germany: Springer, 2006, pp. 260–275.

[9] M. V. B. Delgado and P. P. Mariño, "Using non-uniform probability distribution p* to improve identification performance in dense RFID reader environments," in *Proc. 7th Int. Conf. Innov. Mobile Internet Services Ubiquitous Comput.*, Jul. 2013, pp. 468–471.

[10] A. Baiocchi, D. Garlisi, A. L. Valvo, G. Santaromita, and I. Tinnirello, "'Good to repeat': Making random access near-optimal with repeated contentions," *IEEE Trans. Wireless Commun.*, vol. 19, no. 1, pp. 712–726, Jan. 2020.

[11] N. Cordeschi, F. De Rango, and M. Tropea, "Exploiting an optimal delay-collision tradeoff in CSMA-based high-dense wireless systems," *IEEE/ACM Trans. Netw.*, vol. 29, no. 5, pp. 2353–2366, Oct. 2021.

[12] L. Kleinrock and F. Tobagi, "Packet switching in radio channels: Part I—Carrier sense multiple-access modes and their throughput-delay characteristics," *IEEE Trans. Commun.*, vol. COM-23, no. 12, pp. 1400–1416, Dec. 1975.

[13] P. Huang, L. Xiao, S. Soltani, M. W. Mutka, and N. Xi, "The evolution of MAC protocols in wireless sensor networks: A survey," *IEEE Commun. Surveys Tuts.*, vol. 15, no. 1, pp. 101–120, 1st Quart., 2013.

[14] R. Braun and F. Afroz, "Energy-efficient MAC protocols for wireless sensor networks: A survey," *Int. J. Sensor Netw.*, vol. 32, no. 3, p. 150, 2020.

[15] M. A. Rahman, A. T. Asyhari, I. F. Kurniawan, M. J. Ali, M. M. Rahman, and M. Karim, "A scalable hybrid MAC strategy for traffic-differentiated IoT-enabled intra-vehicular networks," *Comput. Commun.*, vol. 157, pp. 320–328, May 2020.

[16] M. Yang, B. Li, and Z. Yan, "MAC technology of IEEE 802.11ax: Progress and tutorial," *Mobile Netw. Appl.*, vol. 26, no. 3, pp. 1122–1136, Jun. 2021.

[17] O. Sharon and Y. Alpert, "Single user MAC level throughput comparision: IEEE 802.11ax vs. IEEE 802.11ac," *Wireless Sensor Netw.*, vol. 9, no. 5, pp. 166–177, 2017.

[18] N. Ahmed, D. De, F. A. Barbhuiya, and Md. I. Hussain, "MAC protocols for IEEE 802.11ah-based Internet of Things: A survey," *IEEE Internet Things J.*, vol. 9, no. 2, pp. 916–938, Jan. 2022.

[19] A. N. Alvi, S. H. Bouk, S. H. Ahmed, and M. A. Yaqub, "Influence of backoff period in slotted CSMA/CA of IEEE 802.15. 4," in *Proc. Int. Conf. Wired/Wireless Internet Commun.* Thessaloniki, Greece: Springer, 2016, pp. 40–51.

[20] G. Bianchi, "Performance analysis of the IEEE 802.11 distributed coordination function," *IEEE J. Sel. Areas Commun.*, vol. 18, no. 3, pp. 535–547, Mar. 2000.

[21] A. Maatouk, M. Assaad, and A. Ephremides, "Energy efficient and throughput optimal CSMA scheme," *IEEE/ACM Trans. Netw.*, vol. 27, no. 1, pp. 316–329, Feb. 2019.

[22] Y.-W. Kuo and J.-H. Huang, "A CSMA-based MAC protocol for WLANs with automatic synchronization capability to provide hard quality of service guarantees," *Comput. Netw.*, vol. 127, pp. 31–42, Nov. 2017.

[23] J. Choi, S. Byeon, S. Choi, and K. B. Lee, "Activity probability-based performance analysis and contention control for IEEE 802.11 WLANs," *IEEE Trans. Mobile Comput.*, vol. 16, no. 7, pp. 1802–1814, Jul. 2017.

[24] Y. Grunenberger, M. Heusse, F. Rousseau, and A. Duda, "Experience with an implementation of the idle sense wireless access method," in *Proc. ACM CoNEXT Conf. (CoNEXT)*. New York, NY, USA: Association for Computing Machinery, 2007, pp. 1–12.

[25] Y. Yang, J. Wang, and R. Kravets, "Distributed optimal contention window control for elastic traffic in single-cell wireless LANs," *IEEE/ACM Trans. Netw.*, vol. 15, no. 6, pp. 1373–1386, Dec. 2007.

[26] D.-J. Deng, C.-H. Ke, H.-H. Chen, and Y.-M. Huang, "Contention window optimization for ieee 802.11 DCF access control," *IEEE Trans. Wireless Commun.*, vol. 7, no. 12, pp. 5129–5135, Dec. 2008.

[27] Y. Edalat and K. Obraczka, "Dynamically tuning IEEE 802.11's contention window using machine learning," in *Proc. 22nd Int. ACM Conf. Model., Anal. Simulation Wireless Mobile Syst.* New York, NY, USA: Association for Computing Machinery, Nov. 2019, pp. 19–26.

[28] W. Wydmański and S. Szott, "Contention window optimization in IEEE 802.11ax networks with deep reinforcement learning," in *Proc. IEEE Wireless Commun. Netw. Conf. (WCNC)*, Mar. 2021, pp. 1–6.

[29] F. Cali, M. Conti, and E. Gregori, "Dynamic tuning of the IEEE 802.11 protocol to achieve a theoretical throughput limit," *IEEE/ACM Trans. Netw.*, vol. 8, no. 6, pp. 785–799, Dec. 2000.

[30] A. Kumar, E. Altman, D. Miorandi, and M. Goyal, "New insights from a fixed-point analysis of single cell IEEE 802.11 WLANs," *IEEE/ACM Trans. Netw.*, vol. 15, no. 3, pp. 588–601, Jun. 2007.

[31] V. Ramaiyan, A. Kumar, and E. Altman, "Fixed point analysis of single cell IEEE 802.11e WLANs: Uniqueness and multistability," *IEEE/ACM Trans. Netw.*, vol. 16, no. 5, pp. 1080–1093, Oct. 2008.

[32] Z. Cai, M. Lu, and X. Wang, "Randomized broadcast channel access algorithms for ad hoc networks," *Int. J. Wireless Inf. Netw.*, vol. 9, no. 4, pp. 243–258, 2002.

[33] Y. Kawahara and T. Sugiyama, "Priority control method by using non-uniform backoff slot probability in IEEE802.11 WLAN," in *Proc. Int. Conf. Inf. Commun. Technol. Converg. (ICTC)*, Oct. 2019, pp. 38–40.

[34] S. Pudasaini, M. Kang, S. Shin, and J. A. Copeland, "COMIC: Intelligent contention window control for distributed medium access," *IEEE Commun. Lett.*, vol. 14, no. 7, pp. 656–658, Jul. 2010.

[35] O. Raeesi, J. Pirskanen, A. Hazmi, J. Talvitie, and M. Valkama, "Performance enhancement and evaluation of IEEE 802.11ah multi-access point network using restricted access window mechanism," in *Proc. IEEE Int. Conf. Distrib. Comput. Sensor Syst.*, May 2014, pp. 287–293.

[36] *Data Sheet, Chipcon AS SmartRF, 2.4 GHz IEEE 802.15.4/ZigBee-Ready RF Transceiver*, document CC2420, Texas Instrum., Dallas, TX, USA, 2006.

Nicola Cordeschi (Member, IEEE) received the Laurea degree (summa cum laude) in communication engineering and the Ph.D. degree in information and communication engineering from the Sapienza University of Rome in 2004 and 2008, respectively. He was a Fellow Researcher with DIET, Sapienza University of Rome, for ten years, and an Assistant Professor, from 2009 to 2016. Then, he was with DIMES, University of Calabria, and also with the 6G Innovation Centre, University of Surrey, U.K. Since 2022, he has been an Assistant Professor of telecommunication with the Department of Electric and Information Engineering (DEI), Polytechnic University of Bari, Italy. He has authored or coauthored over 80 papers, many of which published in premier network journals and conferences, including IEEE TRANSACTIONS ON MOBILE COMPUTING, IEEE TRANSACTIONS ON VEHICULAR TECHNOLOGY, IEEE TRANSACTIONS ON COMMUNICATIONS, and IEEE/ACM TRANSACTIONS ON NETWORKING. His research interests include adaptive wireless communications, cognitive radio access, medium access control, multi-antenna systems, energy-efficiency, resource management in vehicular communications, grid/cloud computing, distributed computing, cross-layer optimization, mathematical optimization, and game theory. He was a recipient of three best paper awards.

Floriano De Rango (Senior Member, IEEE) received the Graduate degree in computer science and the Ph.D. degree in electronics and telecommunications engineering from the University of Calabria, Cosenza, Italy, in October 2000 and January 2005, respectively. From January 2000 to October 2000, he was with the Telecom Research Laboratory, CSELT, Turin, with a scholarship. From March 2004 to November 2004, he was a Visiting Researcher with the University of California at Los Angeles, Los Angeles, CA, USA. He is currently an Associate Professor with DIMES, University of Calabria. He has authored or coauthored more than 220 papers among international journals and conferences. His research interests include the Internet of Things (IoT), IP QoS architectures, adaptive wireless networks, mobile ad hoc networks, pervasive computing, security, vehicular ad hoc networks, and green networks. In 2009, he has founded a spin-off company (Spintel s.r.l.) in the smart control tools design field for energy efficiency for smart building and cities and the IoT, that won some awards in international competitions, such as the Intel Business Challenge Award. His company has been ranked in the first 20 innovative start-ups in Europe (IBCE 2013). He was a recipient of the Young Researcher Award in 2007.

Andrea Baiocchi received the Laurea degree in electronics engineering and the Ph.D. degree in information and communications engineering from the Sapienza University of Rome in 1987 and 1992, respectively. Since January 2005, he has been a Full Professor with the Department of Information Engineering, Electronics and Telecommunications, Sapienza University of Rome. His research activities have been carried out also in the framework of many national (CNR, MIUR, and POR) and international (European Union and ESA) projects, also taking coordination and responsibility roles. He has published more than 170 papers on international journals and conference proceedings. He is the author of the book *Network Traffic Engineering–Stochastic models and Applications* (Wiley, 2020). His main scientific contributions are on telecommunications network traffic engineering, queuing theory, resource sharing, and congestion control. His current research interests include massive multiple access and vehicular networking. He has participated to the technical program committees of 80 international conferences. He also served in the editorial board of the telecommunications technical journal published by Telecom Italia (currently TIM) for ten years. He is currently an Associate Editor of *Vehicular Communications* (Elsevier).

Open Access funding provided by 'Politecnico di Bari' within the CRUI CARE Agreement